Mechanical characteristics of undisturbed coral gravel soils: the intergranular void ratio as a common governing parameter

Yoichi Watabe
Division of Field Engineering for the Environment
Graduate School of Engineering, Hokkaido University
Kita 13, Nishi 8, Kita-ku, Sapporo 060-8628, Japan
watabe@eng.hokudai.ac.jp

Shinji Sassa
Head of Soil Dynamics Group, Port and Airport Research Institute,
National Institute of Maritime, Port and Aviation Technology
3-1-1 Nagase, Yokosuka 239-0826, Japan

Takashi Kaneko
Soil Mechanics and Geo-environment Group, Port and Airport Research Institute,
National Institute of Maritime, Port and Aviation Technology
3-1-1 Nagae, Yokosuka 239-0826, Japan
National Institute of Maritime, Port and Aviation Technology

Yukio Nakata
Professor of Department of Environmental Geotechnical Engineering,
Yamaguchi University
2-16-1 Tokiwadai Ube 755-8611, Japan

Abstract

Coral gravel soils are composite soils comprising large fragments of finger coral and fine particles of silt matrix. When there is a small amount of coral fragments, the mechanical behavior of the coral gravel soil is mainly governed by the silt matrix, and when there is a large amount of coral fragments, the mechanical behavior is mainly governed by the coral fragments. Undisturbed samples, called high-quality samples in the present study, were collected at large-scale coastal construction sites in Okinawa Prefecture and in Kagoshima Prefecture, Japan. A series of triaxial CD-tests were conducted in the laboratory to evaluate the mechanical characteristics of the coral gravel soils. The test results were examined from various viewpoints, to find a common governing parameter for the mechanical behavior of coral gravel soils. It was anticipated that it would be difficult to interpret the mechanical behaviors of the high-quality samples in a uniform manner because undisturbed coral gravel soils, in the form of natural sediments, are generally very heterogeneous. To provide a reference in parametric interpretation of the test results showing the remarkable features of coral gravel soils, such as interlocking and particle crushing, the test data newly obtained for the high-quality samples were compared to the previous test results obtained for reconstituted mixtures having various volumetric percentages of coral fragments. It was found that an intergranular void ratio corresponding to 0.075 mm, in which particles finer than a grain size of 0.075 mm (i.e., particles of clay and silt) are regarded as voids, can be used as a useful parameter in evaluating the shear strength of both reconstituted and undisturbed coral gravel soil samples.

Keywords:

coral gravel soil, undisturbed sample, coral fragments, silt matrix, particle crush, mechanical properties, triaxial test

1. Introduction

Coral gravel soils are composite soils comprising large fragments of finger coral and fine particles of silt matrix. When there is a small amount of coral fragments, the mechanical behavior of the coral gravel soil is mainly governed by the silt matrix, and when there is a large amount of coral fragments, the mechanical behavior is mainly governed by the coral fragments. In practical design in geotechnical engineering, generally, the shear strength of a low permeable soil is characterized by cohesion, c, corresponding to the undrained shear strength, and the shear strength for a high permeable soil is characterized by shear resistance angle, ϕ, corresponding to the drained shear strength. For coral gravel soils, however, it is very difficult to appropriately judge whether cohesion, c, or shear resistance angle, ϕ, should be used. One of the reasons for this difficulty is sample disturbance due to the existence of coral fragments, which obstruct smooth sampler penetration or coring into the ground. Therefore, the mechanical characteristics of coral gravel soils in the undisturbed state have not been clarified yet. Coral gravel soils are often found in sub-tropical coastal regions, such as the Okinawa Islands in Japan, and determining the shear strength of these soils is one of the major geotechnical issues in these regions.

As a first step to solve this geotechnical issue, the authors (Watabe et al. 2015) previously prepared artificial reconstituted coral gravel soil mixtures with various volumetric percentage of coral gravel fragments and conducted a series of triaxial CU-bar (consolidated and undrained shear with pore pressure measurement) and CD (consolidated and drained shear) tests. From their study, it was clarified that the contact effect (or interlocking) between coral fragments was observed for samples with volumetric percentages of coral gravel fragments larger than a certain classification boundary value (20% in their study), and the shear strength was overestimated in CU-bar tests for samples showing significant dilation because of large amount of coral fragments, in association with unrealistic negative excess pore water pressure in the field conditions. These findings are regarded as

a preliminary step for the present study, whose aim is to study the mechanical behavior of undisturbed samples.

In most site investigations at coastal regions in the Okinawa Islands, soil sampling has been conducted by using conventional soil samplers, such as a thin-walled tube sampler with a core catcher and a fixed piston in the case of clayey soils, and a rotary-type double tube sampler in the case of sandy soils or limestone. Coral gravel soil samples collected at the construction site of the shore road in Urasoe City, Okinawa, are shown in Photo 1. The samples from the surface to a depth of 8 m are coral gravel soils, and samples from deeper than 8 m are limestone. These samples were significantly disturbed because the coral fragments were moved by the sampler edge during sampler penetration.

Because of the difficulty in obtaining good-quality undisturbed samples, as well as ensuring heterogeneity in the material components, the number of studies on the mechanical properties of coral gravel soils has been quite limited. Studies related to the present study, but not on coral gravel soils, have been reported, e.g. studies on composite soils comprising large gravel particles and a fine particle matrix. Fragaszy et al. (1990) studied the particle boundary effect, focusing on the replacement of part of the fine-particle matrix with large gravel particles, and modeled the variation of the soil density as a composite soil package. Fragaszy et al. (1992) and Simoni and Houlsby (2006) evaluated the mechanical properties of sandy soils containing gravel particles. These studies focused on how to evaluate the in situ mechanical properties from laboratory test results using soil specimens with a grain size distribution having a smaller overall average grain size or in which a maximum grain size cut-off was set, when large gravel particles affect the dimensions of the soil specimen.

Kumar and Muir Wood (1999) and Vallejo and Mawby (2000) studied the shear characteristics of composite soils comprising coarse particles and fine particles. These studies commonly concluded that the fine particles governed the shear characteristics when the coarse particle fraction was small, that some effects derived from the coarse particles appeared when the coarse particle fraction was

larger than a certain value, and finally, that the coarse particles governed the shear characteristics when the coarse particle fraction increased further. However, the classification boundary grain size between the domain where fine particles dominate and the domain where coarse particle dominate was reported to be different in these two studies, indicating that the classification boundary depends on the material properties of each soil.

In the case of the coral gravel soils treated in the present study, it is necessary to consider not only the features originating from the soils' composition, namely, composite soils comprising coral fragments and fine particle matrixes, but also the effect of particle crushing. Lade et al. (1996) and Lobo-Guerrero and Vallejo (2005) reported on the effect of particle crushing in sand gravel soils during shear behavior. Recently, the influence of particle crushing in the mechanical behavior of these soils has been examined through computer simulation using the discrete element method (DEM), e.g. in Lobo-Guerrero and Vallejo (2006) and Nakata and Watabe (2015).

As mentioned above, it has been difficult to study the mechanical properties of coral gravel soils because coral fragments hinder the collection of undisturbed soil samples. Recently, however, sampling technology has significantly advanced, and high-quality undisturbed samples can now be collected for coral gravel soils. In Japan, as of today, three types of sampling methods described later have been successfully used for coral gravel soils. In fact, in on-site investigations for large-scale projects and important structures in the Okinawa Islands, coral gravel soils are sometimes collected by using these advanced sampling methods, and these soil samples are used in laboratory tests to determine soil design parameters. In the present study, the advanced sampling method is called high-quality sampling, and the soil samples collected by this method are called high-quality samples.

In the present study, high-quality samples were collected from large-scale coastal construction sites in Okinawa Prefecture (Naha Airport and Naha Port on the main island of Okinawa, Ishigaki Port in Ishigaki Island, Hirara Port in Miyako Island) and in Kagoshima Prefecture (Naze Port in Amami-Oshima Island) and a series of triaxial tests were conducted in the laboratory to evaluate the

mechanical properties of the high-quality samples of coral gravel soils. It was anticipated that uniform interpretation of the mechanical behaviors of the high-quality samples would be difficult because the natural sediment of coral gravel soil is generally very heterogeneous. To provide a reference in a parametric interpretation of the test results, which show the remarkable features of coral gravel soils, such as interlocking and particle crushing, the test data newly obtained for the high-quality samples were compared to the previous test results obtained for reconstituted mixtures having various volumetric percentages of coral fragments in Watabe et al. (2015).

2. Soil samples and test methods

The high-quality samples examined in the present study were collected by one of the high-quality sampling methods mentioned below at Naha Airport, Naha Port, Hirara Port, Ishigaki Port, and Naze Port. These sites are indicated on the map in Fig. 1. Note here that the high-quality sampling methods were originally developed to collect gravely material, particularly at crushed zones. The sampling methods used in the present study were the following three types: Gel-Push sampling (GP sampling, Sakai, 2014), in which a gelled polymer is used to surround the core sample to decrease friction between the core sample and the core tube; Sand Gravel sampling (GS sampling, Hirai et al. 2015), in which muddy water flows out radially from nozzles installed behind a coring cutter to prevent from flushing out the fine particles; and Improved Fresh-Water Core Sampling (IFCS sampling, Kawai et al. 2015) in which muddy water containing fine air bubbles is used to decrease the amount of water to prevent from flushing out the fine particles. The samples from Naha Airport, Naha Port, and Hirara Port (partly) were collected by GP sampling, the samples from Hirara Port (the others) and Ishigaki Port were collected by GS sampling, and the samples from Naze Port were collected by IFCS sampling. It was confirmed that all the samples treated in the present study were in a high-quality state without movement of the coral fragments and flushing out of the fine

particles.

To identify parameters that allow uniform interpretation of the in situ coral gravel soils having large variations in soil properties, brief descriptions of the reconstituted samples having different volumetric percentages of coral fragments treated in Watabe et al. (2015) are also shown here.

A list of the samples examined in the present study is shown in Table 1. The intergranular void ratio ($e_{g0.075}$ and e_{g2}) in the table will be discussed later. The reconstituted coral gravel soils (Table 1a) is a series of composite soils prepared by mixing coral fragments and silt matrixes collected from Urasoe City, Okinawa Prefecture, Japan. Coral fragments with a grain size of 9.5 to 37.5 mm were mixed, at an apparent volumetric percentage of 0 to 44%, into the silt matrix with a water content of 30%, a liquid limit, w_L, of 22.9%, and a non-plastic structure. Note that the longest and shortest dimensions of the coral fragments were measured and the average along with the standard deviation were obtained as 25.9 ± 7.4 mm and 11.0 ± 2.4 mm, respectively. The saturated dry-surface density and dry density of coral fragments was 2350 kg/m^3 (2.35 g/cm^3) and 2110 kg/m^3 (2.11 g/cm^3), respectively, and net particle density of crashed coral fragments was 2760 kg/m^3 (2.76 g/cm^3).

The high-quality samples (Table 1b to 1f) were mainly collected from depths in a range of approximately G.L. –5 to –15 m, corresponding to the overburden effective stress, σ'_{v0}, in a range of approximately 40 to 120 kN/m^2 because the bulk density of the coral gravel soils was approximately 18 kN/m^3. The consolidation pressure in the triaxial test was set to the representative overburden effective stress for the samples, i.e. 50 kN/m^2 for the samples from Naha Airport, Naha Port, Hirara Port, and Naze Port, and 100 kN/m^2 for the samples from Ishigaki Port. Because the triaxial CU-bar test overestimated the shear strength for the samples showing significant negative pore water pressure, which was unrealistic in the field, originating from significant dilation under undrained conditions (Watabe et al. 2015), the series of triaxial tests in the present study was conducted under CD test conditions. The axial strain rate in the shear test was set to 0.1%/min. Excess pore water pressure was not observed during the shear tests, confirming that the tests were conducted under

drained conditions.

X-ray photographs were taken to check the quality of the high-quality samples. A pair of X-ray photographs, taken from two orthogonal lateral directions, of one of the samples collected from Ishigaki Port is shown in Photo 2 as an example. The middle one is a photograph showing the surface of the sample. There are many finger coral fragments surrounded by silt matrix, indicating that the finger coral fragments were not moved and the silt matrix was not flushed away during the coring process, which was performed with a diamond bit in GS sampling.

3. Test results

The results of triaxial CD tests are shown in Figs. 2 to 7. Panels (a) show the relationships between principal stress difference, q (= $\sigma_1 - \sigma_3$), and axial strain, ε_a, and panels (b) show the relationships between volumetric strain, ε_v, and axial strain, ε_a.

In Fig. 2 for the reconstituted samples, the maximum principal stress difference (the peak in the drawings) tends to increase with increasing volumetric percentage of coral fragments. In particular, sample R6, which had the densest package of coral fragments, showed a considerably large maximum principal stress difference.

The samples having volumetric percentages of coral fragments smaller than 10% (samples R1 to R3) showed volume contraction with shearing. The samples having volumetric percentages of the coral fragments of 20% and 30% (samples R4 and R5) showed volume contraction at the beginning, but this changed to a small volume expansion with a further increase in axial strain. The sample with the maximum volumetric percentage of the coral fragments (44%, sample R6) showed significant volume expansion after the small contraction at the beginning. Because of significant soil expansion with shearing, the principal stress difference decreased, i.e., strain softening was observed, after the peak.

In the relationships between the principal stress difference and axial strain (q versus ε_a), very smooth curves were observed for the samples having volumetric percentages of the coral fragments smaller than 10% (samples R1 to R3), whereas jagged curves were observed, corresponding to particle crushing or rearrangement, for the samples having volumetric percentages of the coral fragments larger than 20% (samples R4 to R6). A considerably jagged curve was observed for sample R6 having a volumetric percentage of the coral fragments of 44%, which corresponds to the densest package of the coral fragments.

The stress-strain behavior of the undisturbed coral gravel soils changed markedly with increasing fractions of the coral fragments. Such mechanical characteristics can be summarized as follows. For the samples collected at Naha Airport (Fig. 3), Naha Port (some in Fig. 4) and Naze Port (some in Fig. 7), volume contraction was slightly dominant. Those samples showing contraction tended to exhibit an increase in shear strength corresponding to densification with shear, i.e., strain hardening. For the samples collected at Naha Port (the others in Fig. 4), Naze Port (the others in Fig. 7), Hirara Port (Fig. 5), and Ishigaki Port (Fig. 6), volume expansion was dominant. Those samples showing expansion tended to exhibit a decrease in shear strength corresponding to loosening with shear, i.e. strain softening.

Remarkable site-by-site features are summarized below:

1) For the samples collected at Naha Airport, most of the test results showed strain hardening. The samples having large shear strength showed jagged curves in the diagrams, caused by particle crushing. The strain hardening was caused by volume contraction, i.e., densification, with shear.
2) For the samples collected at Naha Port, some samples, typically sample B4, showed strain hardening, but some other samples, typically samples B5 and B2, which exhibited volume contraction followed by volume expansion, showed strain softening. Note here that for sample B1, the shearing was terminated before reaching the peak strength when the principal stress difference approached the capacity of the load cell.

3) For the samples collected at Hirara Port, all samples showed clear peak strengths and then showed strain softening. After a slight volume contraction at the beginning of shear, the soil behavior turned to volume expansion and the volumetric strain reached between –3% and –6% at an axial strain of 15%. The strain softening can be explained by loosening of the soil package in association with the volume expansion.

4) For the samples collected at Ishigaki Port, most of the samples showed clear peak strengths and then showed strain softening. For the samples that showed considerable strain softening, volume expansion was significant up to between –3% and –6% in volumetric strain at an axial strain of 15%. For some samples, typically samples D4 and D8, peak strength was not clearly observed. These soils were thought to have low density corresponding to the small strength and small volume change. In fact, these soils had relatively larger void ratios, as shown in Table 1e.

5) For the samples collected at Naze Port, most of the samples showed strain softening after the peak in association with volume expansion, but the peak was weaker than that for the samples collected from Hirara Port and Ishigaki Port. For the other samples (samples E2, E7, and E8), strain hardening was observed without a peak in association with the volume contraction with shear. These samples showing volume contraction during shear can be considered to have loose packages; however, the void ratios for these samples in Table 1f are not larger. Because the dilation properties are generally governed by “relative” density, it is difficult to evaluate dilation by using the void ratio or density only.

After completing each triaxial test, the soil was sieved through a 9.5 mm mesh to visualize the coral fragments in the soil specimen. Photo 3 shows the coral fragments included in (a) sample A2 and (b) sample A5 from Naha Airport. In sample A2, all the coral fragments were smaller than 37.5 mm, whereas in sample A5, some coral fragments were larger than 37.5 mm. The volumetric percentages of coral fragments are shown in Table 1, as calculated for all the particles larger than 9.5 mm, as well as for particles between 9.5 and 37.5 mm. It can be assumed that, in the shearing

behavior for the samples including large bodies of coral fragments, shear deformation concentrates at the smaller fragments and silt matrix. Therefore, in the following discussion, the volumetric percentage calculated for the particles smaller than 37.5 mm was used. The coral fragments larger than 37.5 mm are assumed not to contribute to the shear behavior because of their high rigidity, similarly to the cap and pedestal of the triaxial test apparatus.

4. Test results and uniform interpretation

Test results obtained from the triaxial CD tests are shown and discussed in this section. Relationships between the volumetric percentage of coral fragments (horizontal axis) and shear strength parameters (vertical axis): (a) the maximum principal stress difference, q_{max}, (b) the maximum shear resistance angle, ϕ_{max}, and (c) the residual shear resistance angle, ϕ_{res}, are plotted in Fig. 8. Here, in a case without any peak in the variation of ϕ, both the maximum (ϕ_{max}) and the residual (ϕ_{res}) values are defined as the same value as the shear resistance angle, ϕ, at an axial strain of 15%. For the reconstituted samples, it was found that the shear strength increased by interlocking between coral fragments when the volumetric percentage of coral fragments was larger than 20% (Watabe et al. 2015). On the maximum principal stress difference, for the undisturbed samples collected from the field, this tendency was not clear. Only the data regions for the samples collected from Naha Port and Ishigaki Port are overlapped, and show an ambiguous tendency which is consistent with the trend of the data for the reconstituted samples; however, the data were plotted above the data for the reconstituted samples. On the maximum and residual shear resistance angles, it is very difficult to find any tendencies for the data. These data variations for the undisturbed samples are probably caused by non-uniformity of the silt matrix and various dimensions and shapes of the coral fragments. Therefore, the tendency mentioned above was clearly seen only for the reconstituted coral gravel soils comprising the uniform silt matrix and the coral fragments between

9.5 and 37.5 mm. In general, there could be a tendency for shear strength to increase with an increase in the volumetric percentage of coral fragments; however, for the high-quality samples, it was very difficult to see this tendency because of the large variation. Note here that the region where the data for the high-quality samples are plotted is very different from the region where the data for the reconstituted samples are plotted. Most of the data for the high-quality samples were plotted above the trend curve for the reconstituted samples, probably because of the high angularity of the natural coral fragments, as seen in Photo 3. These results indicate a limitation in practical application of the knowledge obtained only from the reconstituted samples in Watabe et al. (2015).

Generally in geotechnical engineering, it is easy to assume that shear strength tends to increase with increasing soil density. Because soil density can be transformed into void ratio, the shear strength could be expressed as a function of void ratio. The relationships between the void ratio, e, (horizontal axis) and shear strength parameters (vertical axis): (a) the maximum principal stress difference, q_{max}, (b) the maximum shear resistance angle, ϕ_{max}, and (c) the residual shear resistance angle, ϕ_{res} are plotted in Fig. 9. The horizontal axis was transformed from volumetric percentage of coral fragments in Fig. 8 into void ratio, e, in Fig. 9. For the reconstituted samples, these shear strength parameters clearly tended to decrease with increasing void ratio in association with loosening in the soil package. These relationships are respectively represented by downward-sloping concave curves. For the high-quality samples, however, it is difficult to find any tendency in the data plots because of the very large data variation, but most of the data are plotted above the trend curve for the reconstituted samples. Only the data for the samples collected from Ishigaki Port show an ambiguous tendency which is consistent with the data trend for the reconstituted samples. This fact can be seen on all the three strength parameters.

In coral gravel soil, the void in the skeletal structure of the coarse particles is filled by the matrix of fine particles. It seems that this composite structure cannot be expressed by the definition of the void ratio, e, normally used in geotechnical engineering. From the above discussion, void ratio, e, is

better than volumetric percentage of coral fragments to explain the maximum principal stress difference, q_{max}; however, some revision is necessary to examine a possibility to explain all the three strength parameters (q_{max}, ϕ_{max}, and ϕ_{max}). In the present study, the concept of intergranular void ratio, e_g (Kuerbis et al., 1988; Georgiannou et al. 1990; Thevanayagam, 1998) was considered. The intergranular void ratio regards the fine particles smaller than a classification boundary as voids, and is used here to evaluate the skeletal structure of the coral gravel soil. To correlate the intergranular void ratio, e_g, to one of the normal soil parameters, the classification boundary between sand and silt at a particle size of 0.075 mm and as the boundary between gravel and sand at a particle size of 2 mm are used here, and expressed as $e_{g0.075}$ and e_{g2}, respectively, to examine the possibility of being a governing parameter for the shear characteristics. The definitions of void ratio, e, and intergranular void ratios ($e_{g0.075}$ and e_{g2}) are illustrated in Fig. 10. In the calculation of normal void ratio e (Fig. 9), net values of particle density excluding intra voids obtained for particles larger (for the samples from Naha Airport, a part of Hirara Port, and a part of Naze Port) and smaller (for all) than 2 mm, respectively, was used in consideration of grain size distribution. These were measured for each soil sample, and obtained as the average along with the standard deviation as 2780 ± 30 kg/m^3 (2.78 ± 0.03 g/cm^3) and 2760 ± 20 kg/m^3 (2.76 ± 0.02 g/cm^3), respectively. To consider the skeletal structure of the coral gravel soil, an apparent particle density corresponding to saturated surface-dry condition should be used in calculation of the intergranular void ratios. In this study, soil particle density in saturated surface-dry condition was measured for many coral fragments and obtained a representative value as 2350 kg/m^3 (2.35 g/cm^3). This representative value was used as the apparent particle density for particles larger than 2 mm in the calculation of intergranular void ratios.

Fig. 9, in which the horizontal axis represents the void ratio, e, was transformed into Figs. 11 and 12, in which the horizontal axes represent the intergranular void ratios, $e_{g0.075}$ and e_{g2}, respectively. In Figs. 11 and 12, data for intergranular void ratios, $e_{g0.075}$ and e_{g2}, larger than 5 and 25, respectively, are outside of the plot area, because these parameters were calculated as unrealistically large values

for the samples with small amounts of coarse particles.

In Fig. 11, with the intergranular void ratio, $e_{g0.075}$, for not only the reconstituted samples but also the high-quality samples, all the strength parameters, namely, (a) the maximum principal stress difference q_{max}, (b) the maximum shear resistance angle, ϕ_{max}, and (c) the residual shear resistance angle, ϕ_{res}, clearly tended to decrease with increasing intergranular void ratio, $e_{g0.075}$, and these relationships are respectively represented by downward-sloping concave curves. In addition, both curves for the reconstituted samples and the high-quality samples are drawn close to each other, particularly on the maximum principal stress difference, indicating that the intergranular void ratio $e_{g0.075}$ can be used as the common governing soil parameter for the three shear strength parameters. Note here that the data range in intergranular void ratio, $e_{g0.075}$, for the high-quality samples are widely plotted along the data range for the reconstituted samples, compared to the fact that the data range in void ratio, e, for each high-quality sample are plotted in a narrow range, particularly the data for the samples collected from Naze Port. This is a notable advantage of the intergranular void ratio, $e_{g0.075}$.

In Fig. 12, with intergranular void ratio, e_{g2}, the strength parameters only for the reconstituted samples clearly tended to decrease with increasing void ratio, and these relationships are respectively represented by downward-sloping concave curves. For the high-quality samples, however, it is difficult to find any tendency in the data plots because of the very large data variation. These are similar to the relationships in Figs. 8 and 9.

As mentioned above, for the reconstituted samples comprising the silt matrix and the coral fragments with controlled grain size distributions, the shear strength parameters (the maximum principal stress difference, q_{max}, the maximum shear resistance angle, ϕ_{max}, and residual shear resistance angle, ϕ_{res}) can be respectively expressed as functions of all four parameters (the volumetric percentage of coral fragments, the void ratio, e, and the intergranular void ratios, $e_{g0.075}$ and e_{g2}). For the high-quality samples collected from the field, however, those shear strength

parameters can be functions of the intergranular void ratio, $e_{g0.075}$. This means that the skeletal structure of the coral gravel soils comprises not only the coral fragments but also the particles of gravel and sand larger than 0.075 mm, and the matrix filling the void of the skeletal structure comprises the clay and silt particles smaller than 0.075 mm. The classification boundary at 0.075 mm in the grain size distribution is consistent with the classification between coarse and fine particles in geotechnical engineering. Either 0.075 mm or 0.050 mm is generally used in the classification of soil particles; however, the conclusion above is not dependent on which definition is used.

In the case of using intergranular void ratio, e_g, if the classification boundary is set at too large a grain size, the calculated intergranular void ratio could be an unrealistically large value because of an insufficient number of large particles for forming the skeletal structure. As an extreme case, if all the particles were smaller than the classification boundary, the calculated intergranular void ratio would be an infinite value. If the intergranular void ratio was calculated to be an unrealistically large value, the assumed classification boundary would not be appropriate for the grain size distribution of the soil. The definition of void ratio, e, generally used in geotechnical engineering is equivalent to the intergranular void ratio, e_g, corresponding to the classification boundary at an infinitesimal value. Void ratio is generally calculated to be a realistic value. On the other hand, the intergranular void ratio could be calculated to be an unrealistically large value if the classification boundary value is set at too large a grain size. Actually, in the present study, the intergranular void ratio with the classification boundary at 2 mm (e_{g2}) was calculated to be an unrealistically large value in some cases. Because coral gravel soils generally comprise both fine particles smaller than 0.075 mm (clay and silt) and coarse particles larger than 0.075 mm (sand and gravel, as well as coral fragments), the intergranular void ratio with the classification boundary at 0.075 mm could be a useful parameter.

5. Practical application

In the present study, through analysis and interpretation of the triaxial CD-test results, it was found that the shear strength parameters (the maximum principal stress difference, q_{max}, the maximum shear resistance angle, ϕ_{max}, and the residual shear resistance angle, ϕ_{res}) could be expressed as functions of the intergranular void ratio, $e_{g0.075}$, with the classification boundary set at 0.075 mm. In this section, one way of using the intergranular void ratio, $e_{g0.075}$, in practice is proposed.

Although the intergranular void ratio, $e_{g0.075}$, could be a common governing parameter for the strength parameters (q_{max}, ϕ_{max}, and ϕ_{res}), their relationships are not perfect, as shown by a certain level of data variation in Fig. 11. Therefore, similarly to general site investigations, laboratory tests for undisturbed samples (called high-quality samples in the present study) are the first priority, but the tests should be triaxial CD tests with a consolidation pressure equivalent to the overburden effective stress for the coral gravel soils because of the high permeability. Then, the test results obtained for the high-quality samples are compared through the intergranular void ratio, $e_{g0.075}$, to confirm whether the results are consistent with the data set previously obtained.

Because high-quality sampling is much more costly than conventional sampling, it is very difficult to conduct high-quality sampling in most construction projects, except some big national projects. Therefore, for samples collected by the conventional method and assumed to be disturbed, first the intergranular void ratio, $e_{g0.075}$, is calculated from the grain size distribution obtained from the samples, and then the shear strength parameters (q_{max}, ϕ_{max}, and ϕ_{res}) are read from the chart shown in Fig. 11. Note here that the value should be read conservatively from the chart in consideration of the data variation.

In real constructions on coral gravel soils, soil parameters representing the mechanical properties have been underestimated, because soil samples are significantly disturbed (Photo 1), resulting in

overdesign in stability evaluation of seawall structure along a reclamation site. Because of overdesign, seawall does not fail in most cases. The above test results and discussion can solve this problem, and to lead an economical design on the basis of fundamental interpretation of mechanical characteristics of coral gravel soils.

6. Conclusions

1) For the coral gravel soil samples showing volume contraction with shear, the relationships between principal stress difference and axial strain obtained from the triaxial CD-tests showed strain hardening corresponding to densification. For the samples showing volume expansion (dilation) with shear, the relationships showed strain softening after the peak strength in the principal stress difference, corresponding to loosening.
2) For the reconstituted samples, when the volumetric percentage of coral fragments with grain sizes of 9.5 to 37.5 mm was larger than 20%, the effect of interlocking and particle crushing was observed in the shearing behavior. However, for the high-quality samples collected from the field, it was very difficult to find a unique relationship between the shear strength parameters (q_{max}, ϕ_{max}, and ϕ_{res}) and the volumetric percentage of coral fragments.
3) In the relationships between shear strength parameters and void ratio, the reconstituted samples had a high correlation; however, the high-quality samples did not have a significant correlation, although all the data for q_{max}, ϕ_{max}, and ϕ_{res} for the high-quality samples were significantly larger than the trend of the data for the reconstituted samples.
4) Intergranular void ratio, $e_{g0.075}$, defined with a classification boundary grain size of 0.075 mm, which assumes that the coarse particles larger than 0.075 mm (sand, and gravel including coral fragments) form a skeletal structure and that the fine particles smaller than 0.075 mm (silt and clay) are regarded as voids, could be a governing parameter for the shear strength parameters,

with a high-correlation. This is consistent with the classification between coarse and fine particles in geotechnical engineering, generally at 0.075 mm or 0.050 mm.

5) Intergranular void ratio, e_{g2}, defined with a classification boundary grain size of 2 mm, which assumes that the particles larger than 2 mm (gravel including coral fragments) form the skeletal structure and that the particles smaller than 2 mm (sand, silt, and clay) are regarded as voids, could not be used a governing parameter for the shear strength parameters with a high-correlation.
6) This is because the void ratio, e, and the intergranular void ratio, e_{g2}, did not have high correlations in the relationships with the shear strength parameters, but the intergranular void ratio, $e_{g0.075}$, did. These facts indicate that there could be an optimum definition of the intergranular void ratio with a certain classification boundary in grain size to find a governing parameter for the shear strength parameters.
7) The intergranular void ratio would be calculated to be an unrealistically large useless value if the classification boundary grain size were set to too large a value. The intergranular void ratio with a classification boundary grain size of 0.075 mm could be a manageable useful parameter because sufficient fractions are classified into both the coarse (sand and gravel including coral fragments forming the skeletal structure) and fine particles (silt and sand forming the matrix).
8) If high-quality samples can be obtained in practice, the shear strength parameters can be effectively determined from the triaxial CD-test results. To improve the reliability of the test results, it is recommended to compare them, by means of the intergranular void ratio, $e_{g0.075}$, with the shear strength dataset previously obtained.
9) If samples are collected by the conventional method and are assumed to be disturbed, the shear strength parameters can be read from the trend curve on the shear strength dataset previously obtained, through the intergranular void ratio, $e_{g0.075}$, calculated from the grain size distribution. The value should be read conservatively from the trend curve in consideration of the data variation.

Note here that the volumetric percentage of coral fragments and void ratios (e, $e_{g0.075}$, and e_{g2}) are calculated for the particles smaller than 37.5 mm.

Acknowledgements

The authors thank Mr. R. Gushi and M. Taira of the Okinawa General Bureau, Cabinet Office, Government of Japan and Mr. K. Arie and S. Moriyama of the Kyushu Regional Development Bureau, Ministry of Land, Infrastructure, Transport and Tourism, Japan for providing the high-quality samples and active discussions on this study from engineering viewpoints. This research work was partly supported by Grant-in-Aid for Scientific Research (No. 23360208) from the Ministry of Education, Culture, Sorts, Science and Technology, Japan.

References

Fragaszy, R.J., Su, W., Siddiqi, F.H., 1990. Effects of oversize particles on the density of clean granular soils. Geotechnical Testing Journal 13(2), 106-114. http://dx.doi.org/10.1520/GTJ10701J. ISSN 0149-6115

Fragaszy, R., Su, J., Siddiqi, F., Ho, C., 1992. Modeling strength of sandy gravel. Journal of Geotechnical Engineering 118(6), 920-935. http://dx.doi.org/10.1061/(ASCE)0733-9410(1992)118:6(920)

Georgiannou, V.N., Burland, J.B., Hight, D.W., 1990. The undrained behaviour of clayey sands in triaxial compression and extension. Géotechnique 40(3), 431-449. http://dx.doi.org/10.1680/geot.1990.40.3.431

Hirai, K., Kiku, H., Oshima, A., Rito, F., 2015. GS sampling: A sampling method that minimizes disturbance and compensates for weak point. Journal of Japanese Geotechnical Society 63(4), 10-13. (in Japanese).

Kawai, H., Sonoda, S., Watabe, Y., Matsumoto, S., Ikeda, S., Takada, M., Kitamura, R., 2015. New

sampling method and mechanical property for undisturbed soil with coral gravel. Japanese Geotechnical Journal 10(3), 415-424. (in Japanese) http://dx.doi.org/10.3208/jgs.10.415

Kuerbis, R., Negussey, D., Vaid, Y.P., 1988. Effect of gradation and fine content on the undrained response of sand. Hydraulic fill structure, Geotechnical Special Publication 21, ASCE, New York, 330-345.

Kumar, G.V., Muir Wood, D., 1999. Fall cone and compression tests on clay±gravel mixtures. Géotechnique 49(6), 727-739. http://dx.doi.org/10.1680/geot.1999.49.6.727

Lade, P., Yamamuro, J., Bopp, P., 1996. Significance of particle crushing in granular materials. Journal of Geotechnical Engineering 122(4), 309-316. http://dx.doi.org/10.1061/(ASCE)0733-9410(1996)122:4(309)

Lobo-Guerrero, S., Vallejo, L.E., 2005. DEM analysis of crushing around driven piles in granular materials. Géotechnique 55(8), 617-623. http://dx.doi.org/10.1680/geot.2005.55.8.617

Lobo-Guerrero, S., Vallejo, L.E., 2006. Modeling granular crushing in ring shear tests: experimental and numerical analyses. Soils and Foundations 46(2), 147-157. http://dx.doi.org/10.3208/sandf.46.147

Nakata, Y., Watabe, Y., 2015. Compression behavior for assembly of DEM crushable cylindrical gravels. Geomechanics from Micro to Macro, Proceedings of the International Symposium on Geomechanics from Micro to Macro, IS-Cambridge 2014, 281-284. http://dx.doi.org/10.1201/b17395-49

Sakai, K., 2014. GP sampling. Journal of Japanese Geotechnical Society 62(10), 37-38. (in Japanese)

Simoni, A., Houlsby, G.T., 2006. The direct shear strength and dilatancy of sand–gravel mixtures. Geotechnical and Geological Engineering 24(3), 523-549. http://dx.doi.org/10.1007/s10706-004-5832-6

Thevanayagam, S., 1998. Effect of fines and confining stress on undrained shear strength of silty sands. Journal of Geotechnical and Geoenvironmental Engineering 124(6), 479-491.

http://dx.doi.org/10.1061/(ASCE)1090-0241(1998)124:6(479)

Vallejo, L.E., Mawby, R., 2000. Porosity influence on the shear strength of granular material-clay mixtures. Engineering Geology 58(2), 125-136. http://dx.doi.org/10.1016/S0013-7952(00)00051-X

Watabe, Y., Sassa, S., Kaneko, T., Nakata, Y., 2015. Mechanical characteristics of reconstituted coral gravel soils with different fractions of finger-coral fragments and silt matrix. Soils and Foundations 55(5), 1233-1242. http://dx.doi.org/10.1016/j.sandf.2015.09.022

List of Tables, Figures, and Photos

Fig. 2. Results of the triaxial CD-test for the reconstituted samples: (a) relationships between principal stress difference, q (= $\sigma_1 - \sigma_3$), and axial strain, ε_a, and (b) relationships between volumetric strain, ε_v, and axial strain ε_a.

Fig. 3. Results of the triaxial CD-test for the high-quality samples from Naha Airport: (a) relationships between principal stress difference, q (= $\sigma_1 - \sigma_3$), and axial strain, ε_a, and (b) relationships between volumetric strain, ε_v, and axial strain, ε_a.

Fig. 4. Results of the triaxial CD-test for the high-quality samples from Naha Port: (a) relationships between principal stress difference, q (= $\sigma_1 - \sigma_3$), and axial strain, ε_a, and (b) relationships between volumetric strain, ε_v, and axial strain, ε_a.

Fig. 5. Results of the triaxial CD-test for the high-quality samples from Hirara Port: (a) relationships between principal stress difference, q (= $\sigma_1 - \sigma_3$), and axial strain, ε_a, and (b) relationships between volumetric strain, ε_v, and axial strain, ε_a.

Fig. 6. Results of the triaxial CD-test for the high-quality samples from Ishigaki Port: (a) relationships between principal stress difference, q (= $\sigma_1 - \sigma_3$), and axial strain, ε_a, and (b) relationships between volumetric strain, ε_v, and axial strain, ε_a.

Fig. 7. Results of the triaxial CD-test for the high-quality samples from Naze Port: (a) relationships between principal stress difference, q (= $\sigma_1 - \sigma_3$), and axial strain, ε_a, and (b) relationships between volumetric strain, ε_v, and axial strain, ε_a.

Fig. 8. Relationships between volumetric percentage of coral fragments (horizontal axis) and shear strength parameters (vertical axis): (a) the maximum principal stress difference, q_{max}, (b) the maximum shear resistance angle, ϕ_{max}, and (c) the residual shear resistance angle, ϕ_{res}.

Fig. 9. Relationships between void ratio, e, (horizontal axis) and shear strength parameters (vertical axis): (a) the maximum principal stress difference, q_{max}, (b) the maximum shear resistance angle, ϕ_{max}, and (c) the residual shear resistance angle, ϕ_{res}.

Fig. 10. Definitions of void ratio (e) and intergranular void ratio ($e_{g0.075}$ and e_{g2}).

Fig. 11. Relationships between and intergranular void ratio $e_{g0.075}$ (horizontal axis) and shear strength parameters (vertical axis): (a) the maximum principal stress difference, q_{max}, (b) the maximum shear resistance angle, ϕ_{max}, and (c) the residual shear resistance angle, ϕ_{res}.

Fig. 12. Relationships between the intergranular void ratio e_{g2} (horizontal axis) and shear strength parameters (vertical axis): (a) the maximum principal stress difference, q_{max}, (b) the maximum shear resistance angle, ϕ_{max}, and (c) the residual shear resistance angle, ϕ_{res}.

Photo 1. Coral gravel soil samples collected from Urasoe City, Okinawa, Japan, by conventional method: (a) G.L. –0.45 m to G.L. –4.45 m, and (b) G.L. –5.45 m to G.L. –9.40 m.

Photo 2. X-ray photograph of high-quality sample D2 from Ishigaki Port.

Photo 3. The coral fragments larger than 9.5 mm sieved from high-quality samples: (a) sample A2 and (b) sample A5 from Naha Airport.

Sample ID	Symbol	Volumetric percentage of coral fragments > 9.5 mm (%)	Volumetric percentage of coral fragments > 9.5 mm and < 37.5 mm (%)	Percentage finer by weight < 9.5 mm (%)	Percentage finer by weight < 2 mm (%)	Percentage finer by weight < 0.075 mm (%)	Void ratio e_0	Intergranular void ratio	
								$e_{g0.075}$	e_{g2}
C0S100	R1	0	0	100.0	100.0	48.2	0.98	2.82	∞
C5S95	R2	5	5	93.1	93.1	44.9	0.86	2.33	19.94
C10S90	R3	10	10	86.6	86.6	41.8	0.77	1.98	9.58
C20S80	R4	20	20	74.1	74.1	35.7	0.67	1.52	4.30
C30S70	R5	30	30	62.5	62.5	30.2	0.51	1.12	2.51
C44S56	R6	44	44	47.6	47.6	23.0	0.42	0.81	1.43

Sample ID	Depth from G.L. (m)	Symbol	Volumetric percentage of coral fragments > 9.5 mm (%)	Volumetric percentage of coral fragments * > 9.5 mm and < 37.5 mm (%)	Percentage finer by weight * < 9.5 mm (%)	Percentage finer by weight * < 2 mm (%)	Percentage finer by weight * < 0.075 mm (%)	Void ratio * e_0	Intergranular void ratio *	
									$e_{g0.075}$	e_{g2}
GP1-3	5.75	A1	8.0	8.0	88.7	80.4	57.3	0.80	3.04	7.11
GP1-6	10.48	A2	10.7	10.7	84.5	76.7	39.3	0.80	1.90	5.90
GP1-7	11.48	A3	2.4	2.4	96.2	84.1	41.7	0.94	2.27	9.76
GP1-9	13.40	A4	17.8	10.6	85.4	79.9	42.1	0.57	1.63	5.83
GP2′-6	10.85	A5	20.8	8.4	88.0	72.1	23.9	0.79	1.31	4.74
GP2′-7	11.25	A6	26.9	14.1	77.5	62.7	17.9	0.96	1.36	3.79

* Calculated without particles larger than 37.5 mm

Sample ID	Depth from G.L. (m)	Symbol	Volumetric percentage of coral gravels > 9.5 mm (%)	Volumetric percentage of coral gravels * > 9.5 mm and <37.5 mm (%)	Percentage finer by weight * < 9.5 mm (%)	Percentage finer by weight * < 2 mm (%)	Percentage finer by weight * <0.075 mm (%)	Void ratio * e_0	Intergranular void ratio *	
									$e_{g0.075}$	e_{g2}
1-3.80	3.80	B1	25.5	21.8	67.7	34.8	9.6	0.72	0.89	1.51
1-5.77	5.77	B2	26.8	23.5	63.4	54.7	11.4	0.86	1.09	2.80
1-12.0	12.0	B3	2.2	2.2	96.4	85.0	20.0	0.98	1.46	10.79
3-11.3	11.3	B4	19.7	15.1	74.1	62.0	17.3	1.08	1.50	4.01
3-13.8	13.8	B5	1.0	1.0	98.4	83.9	6.7	1.01	1.15	9.99

* Calculated without particles larger than 37.5 mm

Sample ID	Depth from G.L. (m)	Symbol	Volumetric percentage of coral gravels > 9.5 mm (%)	Volumetric percentage of coral gravels * > 9.5 mm and <37.5 mm (%)	Percentage finer by weight * < 9.5 mm (%)	Percentage finer by weight * < 2 mm (%)	Percentage finer by weight * <0.075 mm (%)	Void ratio * e_0	Intergranular void ratio *	
									$e_{g0.075}$	e_{g2}
G8-A	11.46	C1	0.2	0.2	99.7	97.4	17.2	0.93	1.32	61.88
G8-C	14.86	C2	0.1	0.1	99.9	97.9	14.1	1.00	1.32	78.15
G9-1	14.05	C3	1.7	1.7	97.5	93.6	13.0	0.92	1.20	24.85
G11-1	13.50	C4	14.9	13.3	81.9	70.6	19.8	0.70	1.09	4.15
G11-A	15.21	C5	37.6	7.1	89.8	80.9	26.6	0.84	1.47	7.46
G11-C	15.61	C6	25.1	13.3	80.2	72.1	25.3	0.86	1.45	4.93
G1-2-1-1	2.30	C7	18.0	18.0	74.7	48.7	9.3	0.70	0.85	2.06
G1-2-1-2	2.30	C8	9.8	9.8	85.4	57.6	9.5	0.82	0.99	2.90
G1-4-3-7	16.60	C9	2.8	2.8	95.9	89.0	14.1	0.90	1.21	14.1
G2-1-2-8	16.60	C10	0.0	0.0	100	98.7	13.2	0.96	1.25	123.24

* Calculated without particles larger than 37.5 mm

Sample ID	Depth from G.L. (m)	Symbol	Volumetric percentage of coral gravels > 9.5 mm (%)	Volumetric percentage of coral gravels * > 9.5 mm and < 37.5 mm (%)	Percentage finer by weight * < 9.5 mm (%)	Percentage finer by weight * < 2 mm (%)	Percentage finer by weight * < 0.075 mm (%)	Void ratio e_0*	Intergranular void ratio *	
									$e_{g0.075}$	e_{g2}
GS-4	10.68	D1	43.2	30.2	60.7	52.4	13.9	0.58	0.82	2.05
GS-5	11.86	D2	11.7	11.7	84.6	69.7	25.9	0.64	1.17	3.82
GS-6	12.52	D3	8.3	8.3	88.6	76.9	41.1	0.74	1.88	5.61
GS-8	14.50	D4	9.4	9.4	87.0	76.2	45.9	0.73	2.10	5.44
GS-9	15.50	D5	7.7	7.7	89.8	80.8	51.5	0.68	2.35	6.70
GS-10	16.51	D6	10.6	10.6	85.8	76.2	44.7	0.69	1.95	5.26
GS-11	17.51	D7	8.0	8.0	89.3	83.0	53.5	0.71	2.55	7.76
GS-12	18.84	D8	9.7	9.7	86.8	82.3	56.9	0.73	2.86	7.56
GS-13	11.48	D9	21.5	21.5	72.5	58.0	24.7	0.56	1.02	2.39
GS-14	12.50	D10	14.0	14.0	81.6	67.4	39.9	0.63	1.62	3.48

* Calculated without particles larger than 37.5 mm

Sample ID	Depth from G.L. (m)	Symbol	Volumetric percentage of coral gravels > 9.5 mm (%)	Volumetric percentage of coral gravels * > 9.5 mm and < 37.5 mm (%)	Percentage finer by weight * < 9.5 mm (%)	Percentage finer by weight * < 2 mm (%)	Percentage finer by weight * < 0.075 mm (%)	Void ratio * e_0	Intergranular void ratio *	
									$e_{g0.075}$	e_{g2}
3-I-2	3.00	E1	0.2	0.2	99.7	97.6	11.9	1.00	1.28	37.35
3-I-3	4.50	E2	3.2	3.2	95.4	95.0	80.8	0.86	8.37	30.97
3-I-4	6.00	E3	5.9	5.9	89.8	87.7	68.8	1.24	5.85	14.67
3-S-5	7.50	E4	0.1	0.1	99.9	99.2	71.1	0.93	5.65	199.84
3-I-6-1	9.00	E5	0.4	0.4	99.4	98.3	73.0	0.88	5.92	91.41
3-I-7-1	10.50	E6	0.1	0.1	99.9	98.0	71.8	0.98	5.98	83.81
4-I-5	17.50	E7	14.9	14.9	80.2	70.6	48.1	0.65	2.05	4.03
5-I-8	12.00	E8	12.0	12.0	82.6	74.6	64.6	0.84	3.81	5.42

* Calculated without particles larger than 37.5 mm

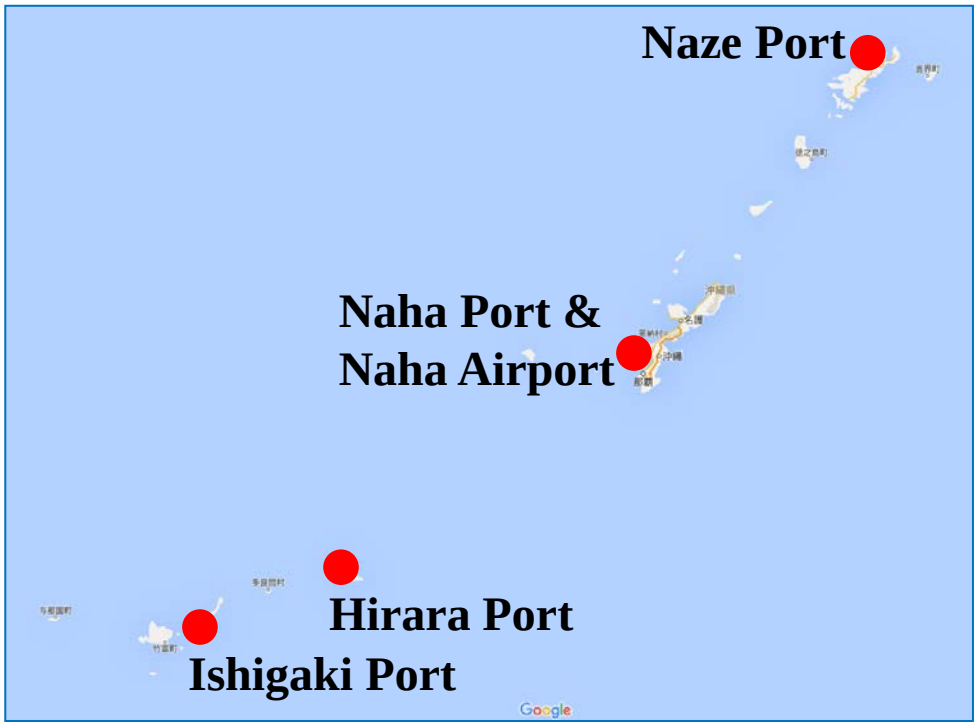
Naze Port
Naha Port &
Naha Airport
Hirara Port
Ishigaki Port
Google


Japan
北朝鮮
大韓民国
日本
東京
大阪
名古屋
広島
福岡
札幌
日本海
東シナ海
黄海
Google

a

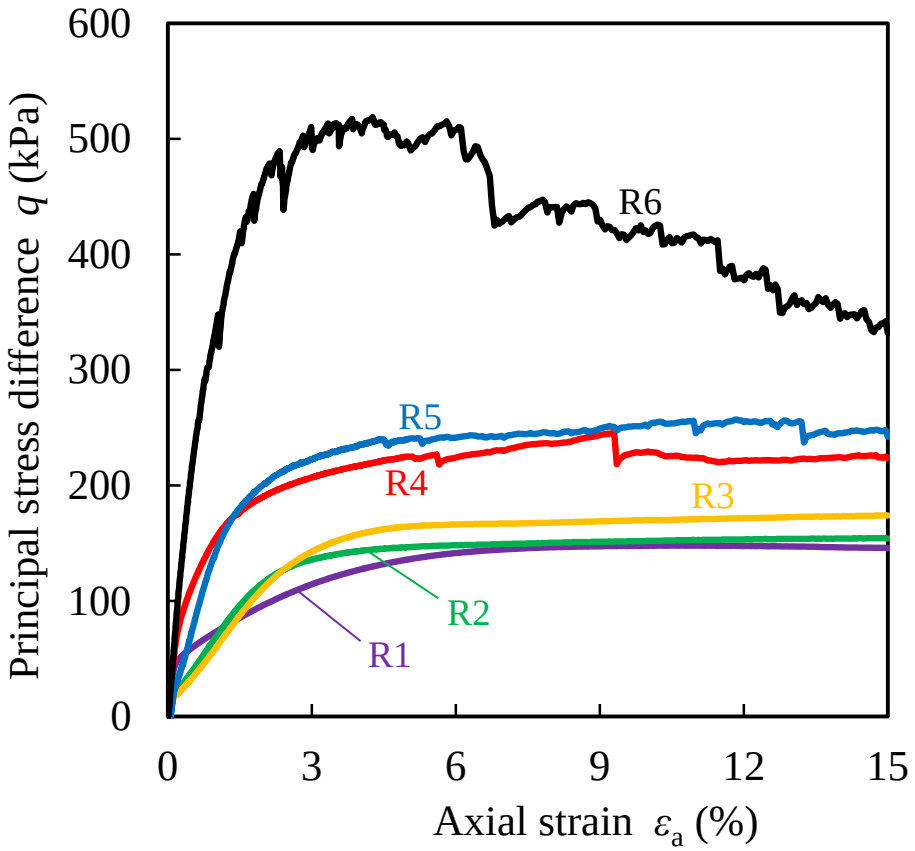
600
500
400
300
200
100
0
Principal stress difference q (kPa)
R6
R5
R4
R3
R2
R1
0
3
6
9
12
15
Axial strain ε_a (%)

b

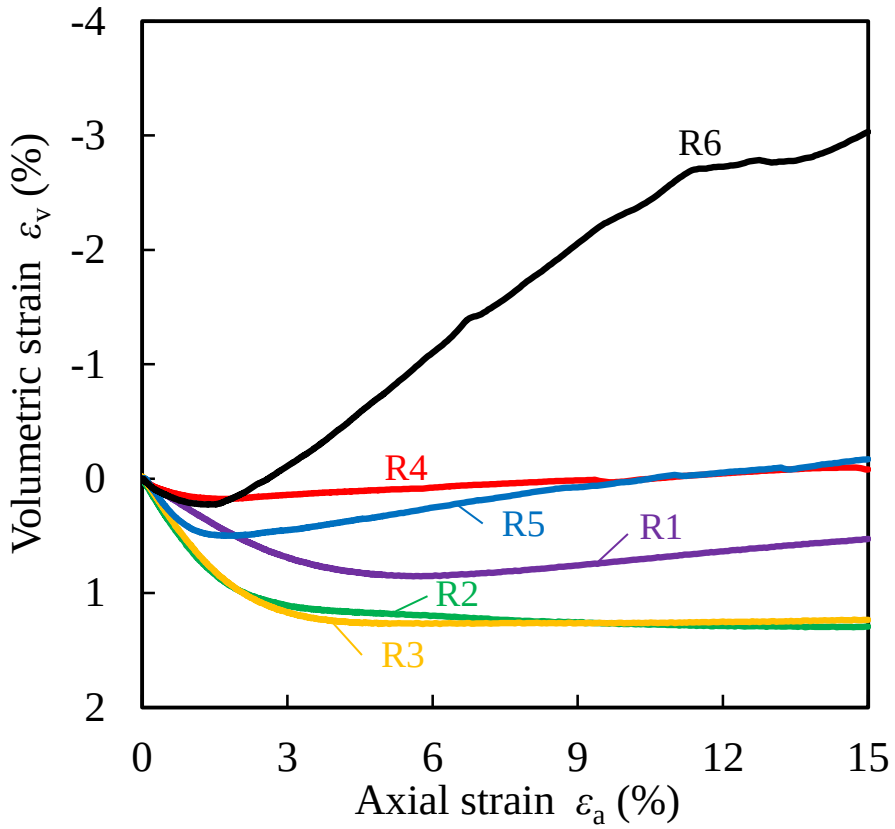
-4
-3
-2
-1
0
1
2
Volumetric strain ε_v (%)
R6
R4
R5
R1
R2
R3
0
3
6
9
12
15
Axial strain ε_a (%)

a

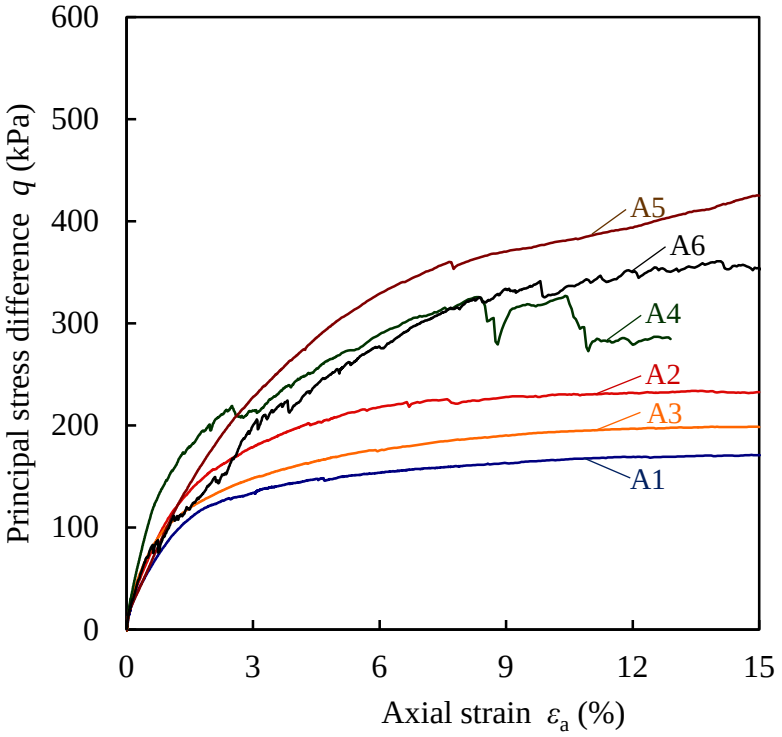
Principal stress difference q (kPa)
600
500
400
300
200
100
0
0
3
6
9
12
15
Axial strain εa (%)
A5
A6
A4
A2
A3
A1

b

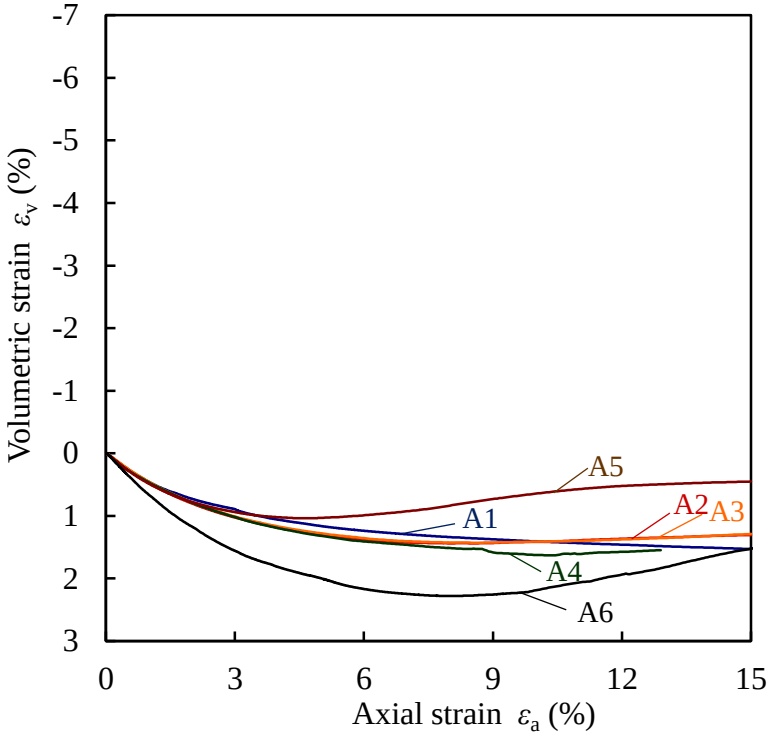
Volumetric strain εv (%)
-7
-6
-5
-4
-3
-2
-1
0
1
2
3
0
3
6
9
12
15
Axial strain εa (%)
A5
A1
A2
A3
A4
A6

a

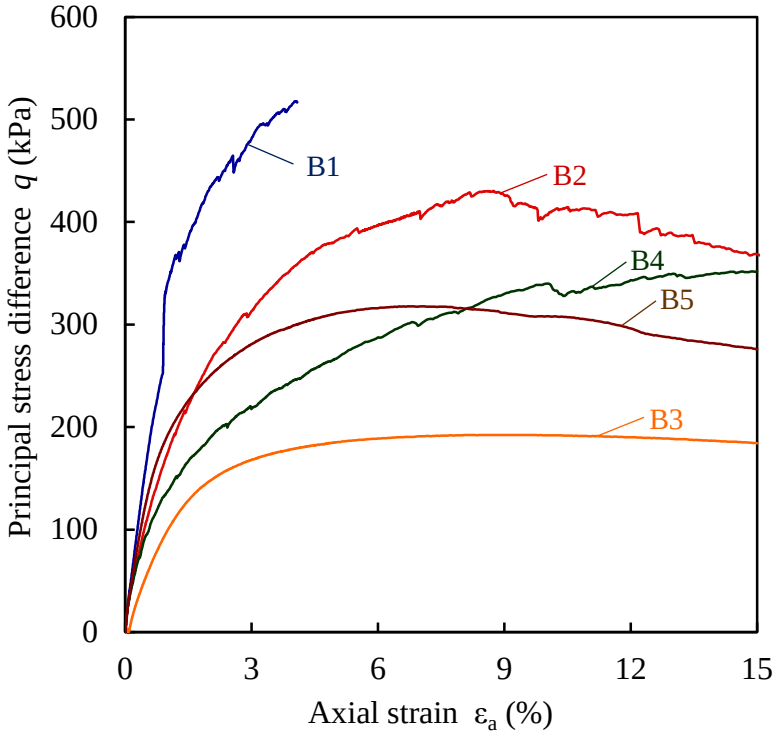
Principal stress difference q (kPa)
600
500
400
300
200
100
0
0
3
6
9
12
15
Axial strain εa (%)
B1
B2
B4
B5
B3

b

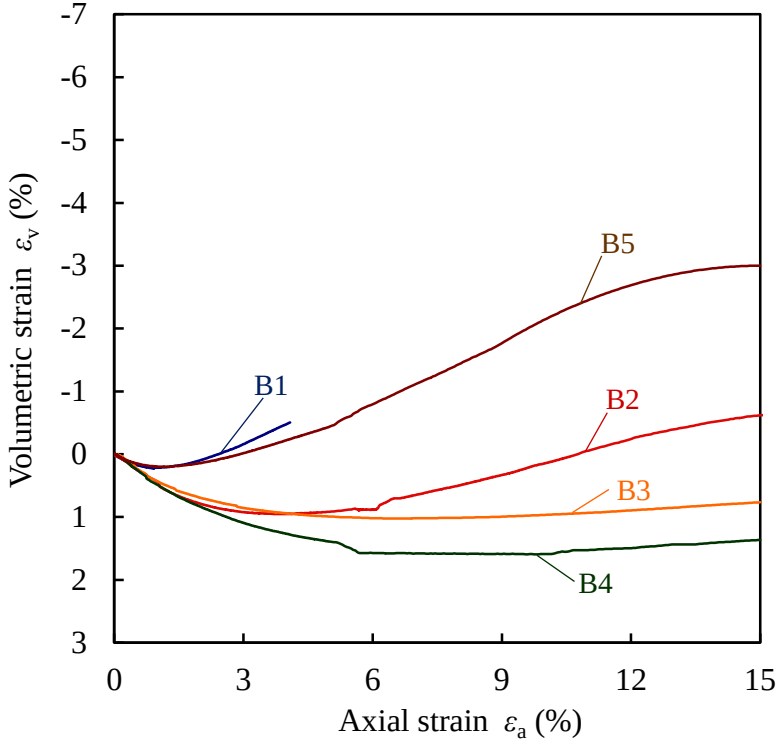
Volumetric strain εv (%)
-7
-6
-5
-4
-3
-2
-1
0
1
2
3
0
3
6
9
12
15
Axial strain εa (%)
B5
B1
B2
B3
B4

a

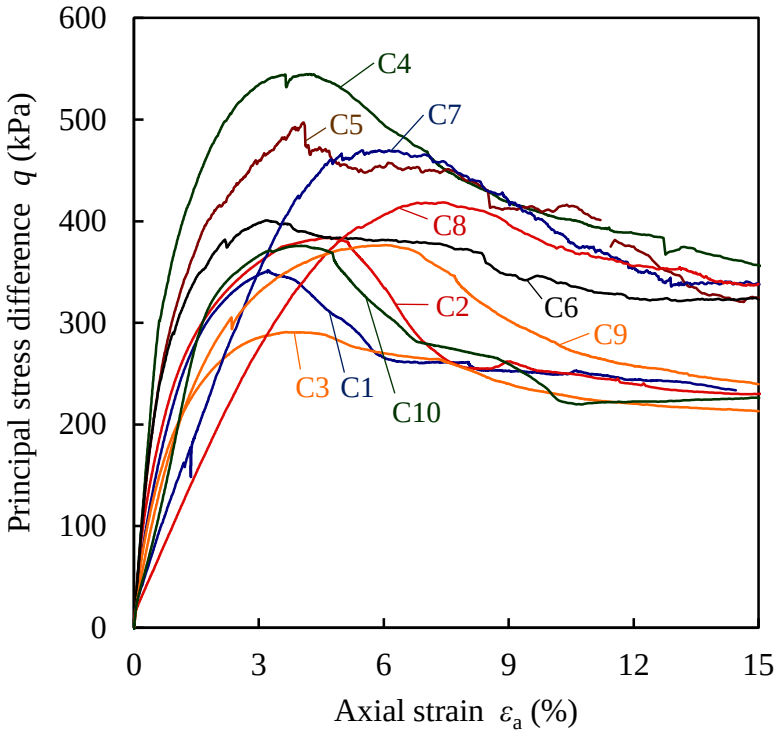
Principal stress difference q (kPa)
600
500
400
300
200
100
0
0
3
6
9
12
15
Axial strain εa (%)
C4
C5
C7
C8
C2
C6
C9
C3
C1
C10

b

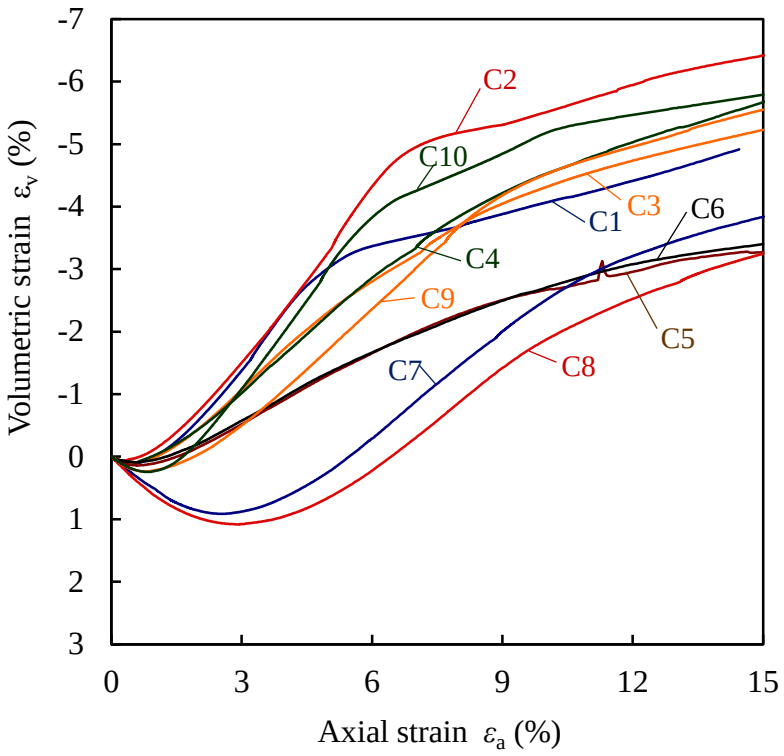
Volumetric strain εv (%)
-7
-6
-5
-4
-3
-2
-1
0
1
2
3
0
3
6
9
12
15
Axial strain εa (%)
C2
C10
C3
C1
C6
C4
C9
C5
C7
C8

a

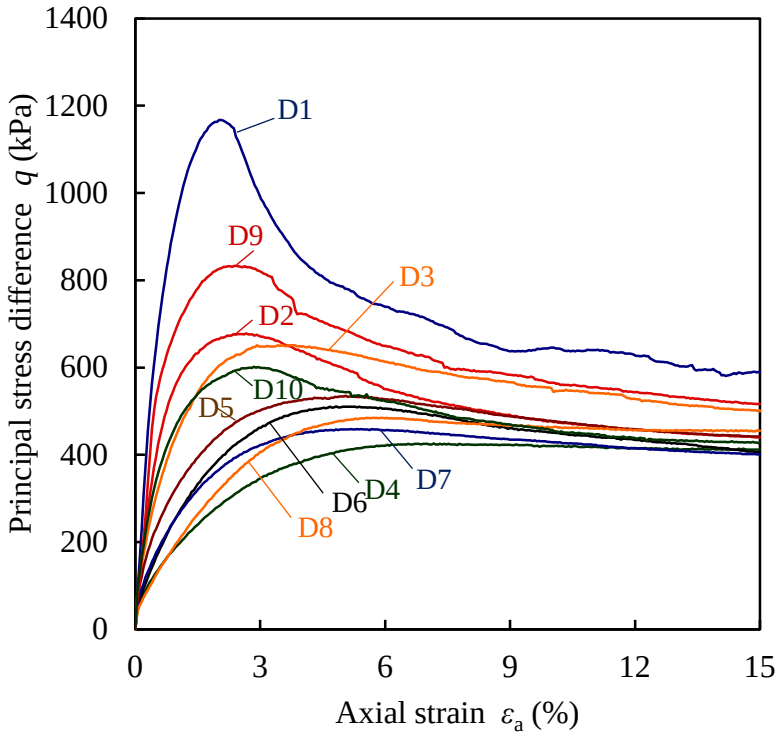
Principal stress difference q (kPa)
1400
1200
1000
800
600
400
200
0
0
3
6
9
12
15
Axial strain εa (%)
D1
D9
D3
D2
D5
D10
D6
D4
D7
D8

b

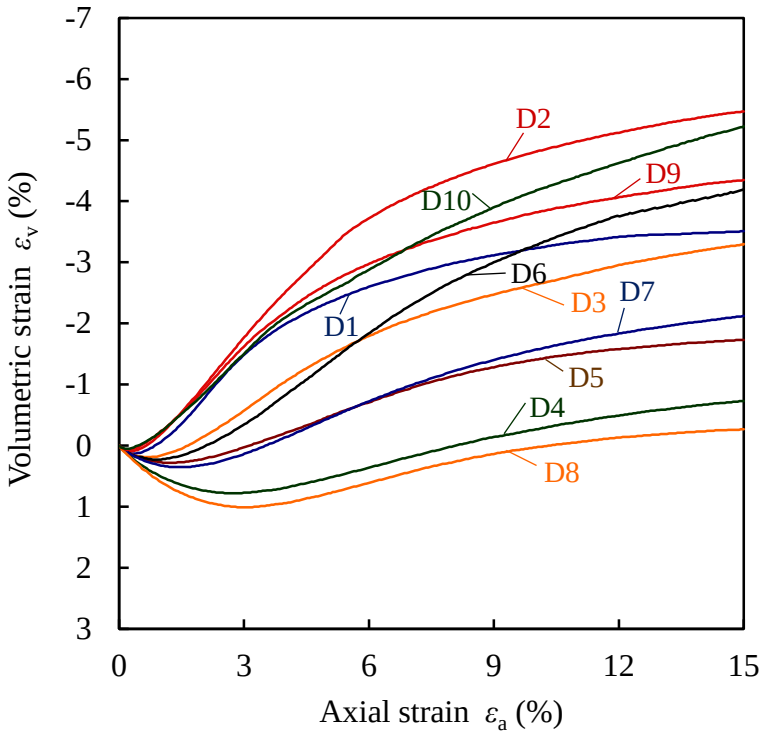
Volumetric strain εv (%)
-7
-6
-5
-4
-3
-2
-1
0
1
2
3
0
3
6
9
12
15
Axial strain εa (%)
D2
D9
D10
D6
D3
D7
D1
D5
D4
D8

a

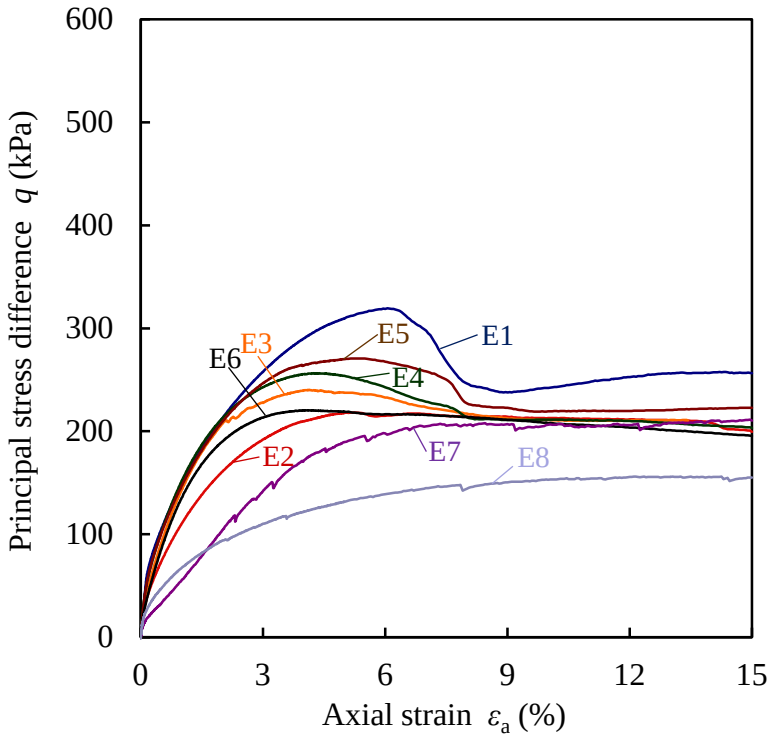
Principal stress difference q (kPa)
600
500
400
300
200
100
0
0
3
6
9
12
15
Axial strain εa (%)
E1
E2
E3
E4
E5
E6
E7
E8

b

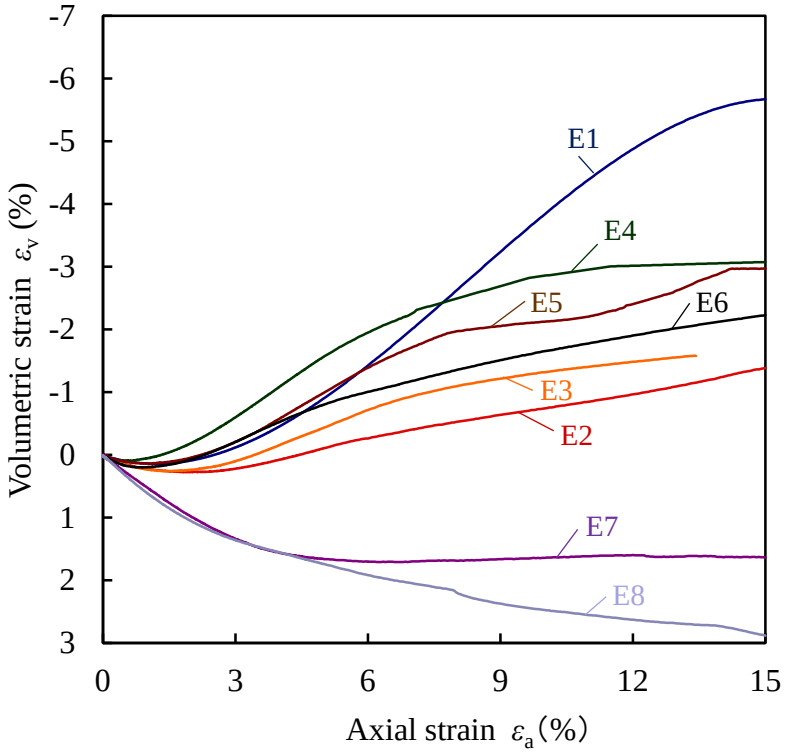
Volumetric strain εv (%)
-7
-6
-5
-4
-3
-2
-1
0
1
2
3
0
3
6
9
12
15
Axial strain εa (%)
E1
E2
E3
E4
E5
E6
E7
E8

a

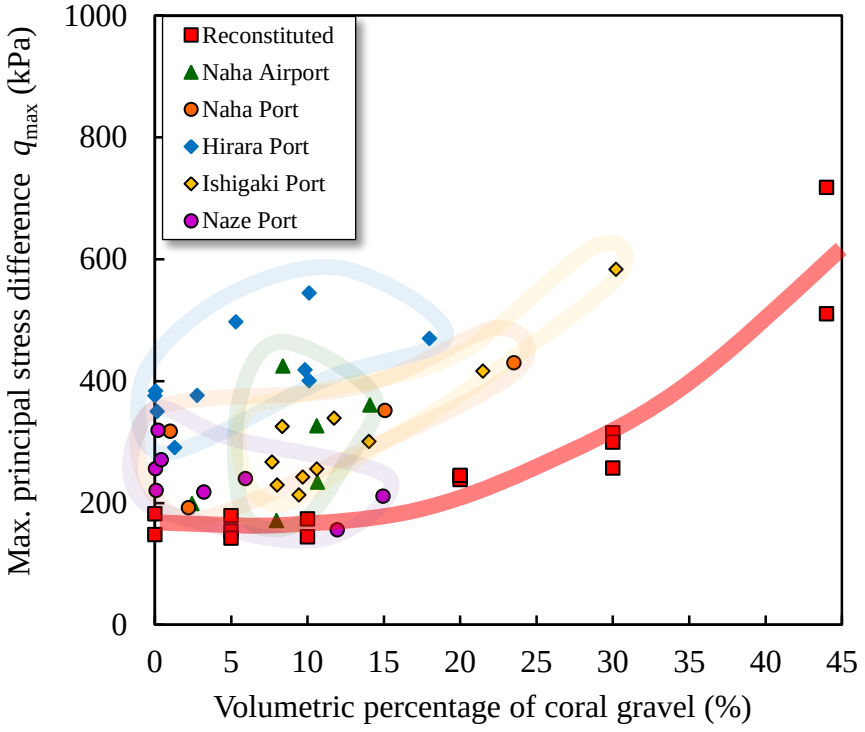
Max. principal stress difference q_{max} (kPa)
1000
800
600
400
200
0
0
5
10
15
20
25
30
35
40
45
Volumetric percentage of coral gravel (%)
Reconstituted
Naha Airport
Naha Port
Hirara Port
Ishigaki Port
Naze Port

b

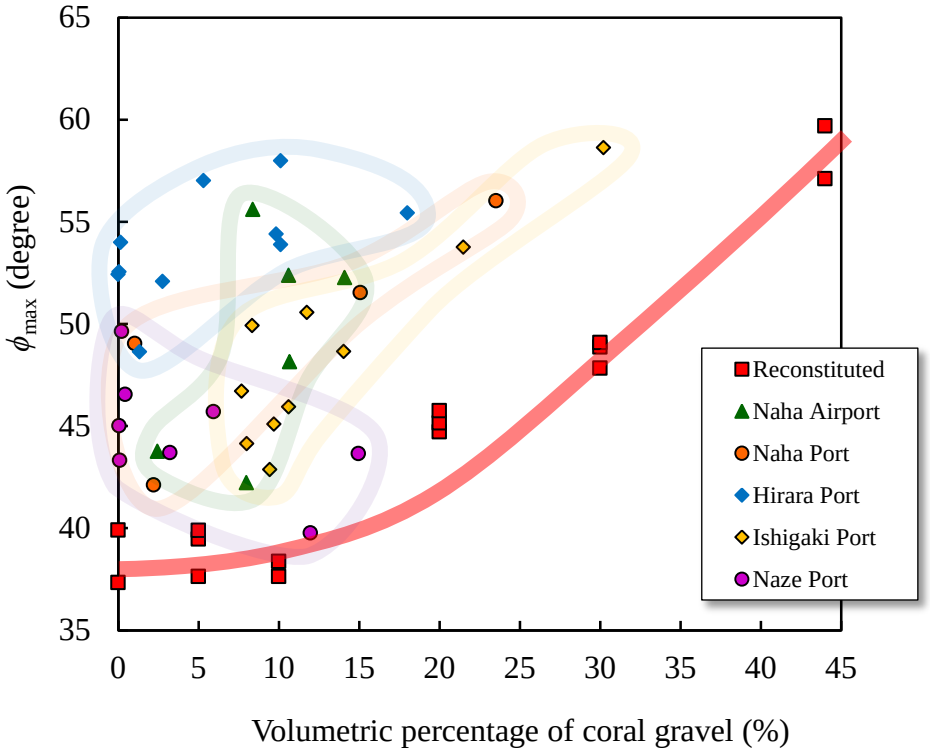
ϕ_{max} (degree)
65
60
55
50
45
40
35
0
5
10
15
20
25
30
35
40
45
Volumetric percentage of coral gravel (%)
Reconstituted
Naha Airport
Naha Port
Hirara Port
Ishigaki Port
Naze Port

c

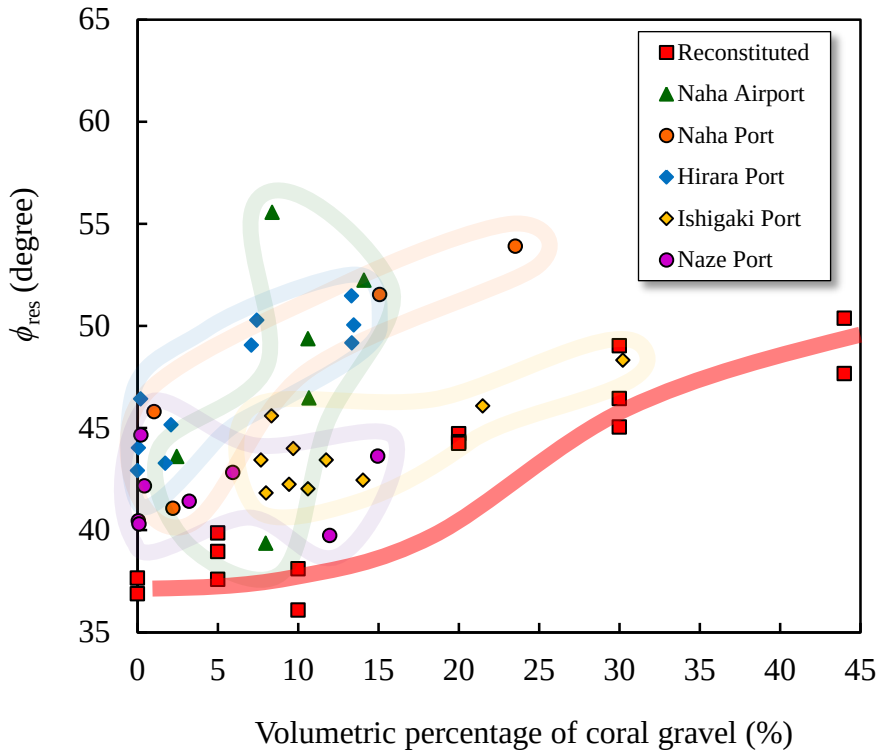
65
60
55
50
45
40
35
ϕ_{res} (degree)
0
5
10
15
20
25
30
35
40
45
Volumetric percentage of coral gravel (%)
Reconstituted
Naha Airport
Naha Port
Hirara Port
Ishigaki Port
Naze Port

a

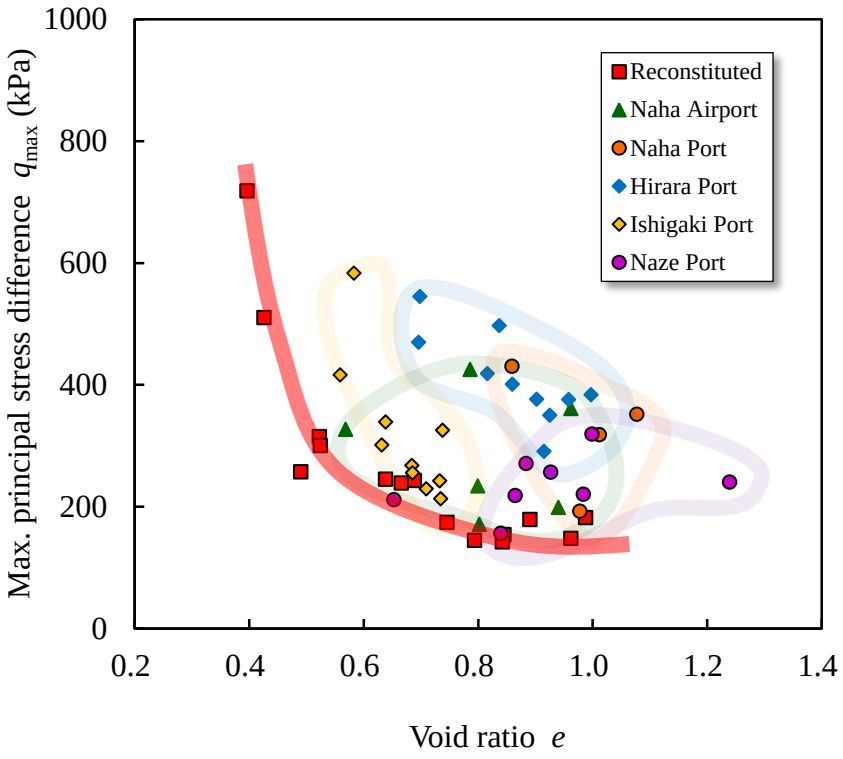
Max. principal stress difference q_{max} (kPa)
1000
800
600
400
200
0
0.2
0.4
0.6
0.8
1.0
1.2
1.4
Void ratio e
Reconstituted
Naha Airport
Naha Port
Hirara Port
Ishigaki Port
Naze Port

b

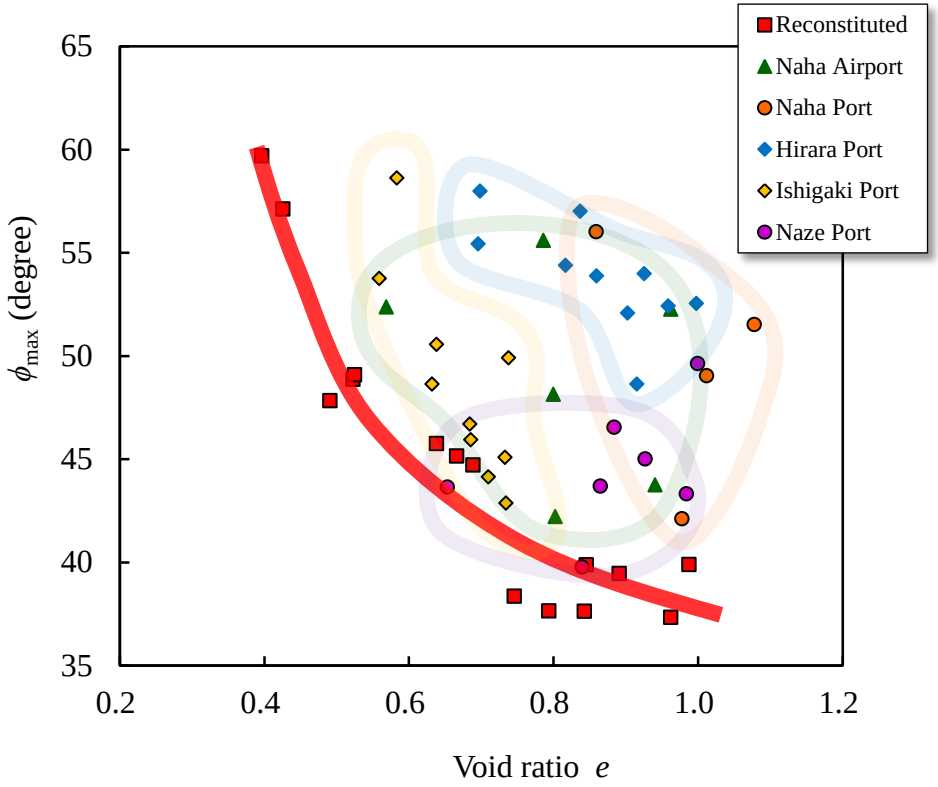
ϕ_{max} (degree)
65
60
55
50
45
40
35
0.2
0.4
0.6
0.8
1.0
1.2
Void ratio e
Reconstituted
Naha Airport
Naha Port
Hirara Port
Ishigaki Port
Naze Port

c

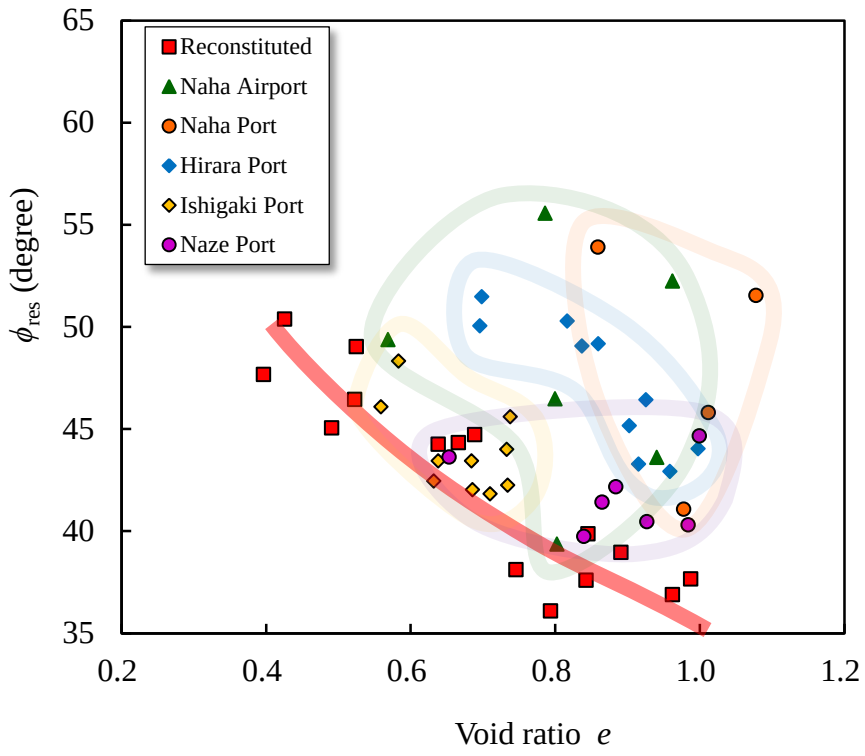
Reconstituted
Naha Airport
Naha Port
Hirara Port
Ishigaki Port
Naze Port
65
60
55
50
45
40
35
ϕ_{res} (degree)
0.2
0.4
0.6
0.8
1.0
1.2
Void ratio e

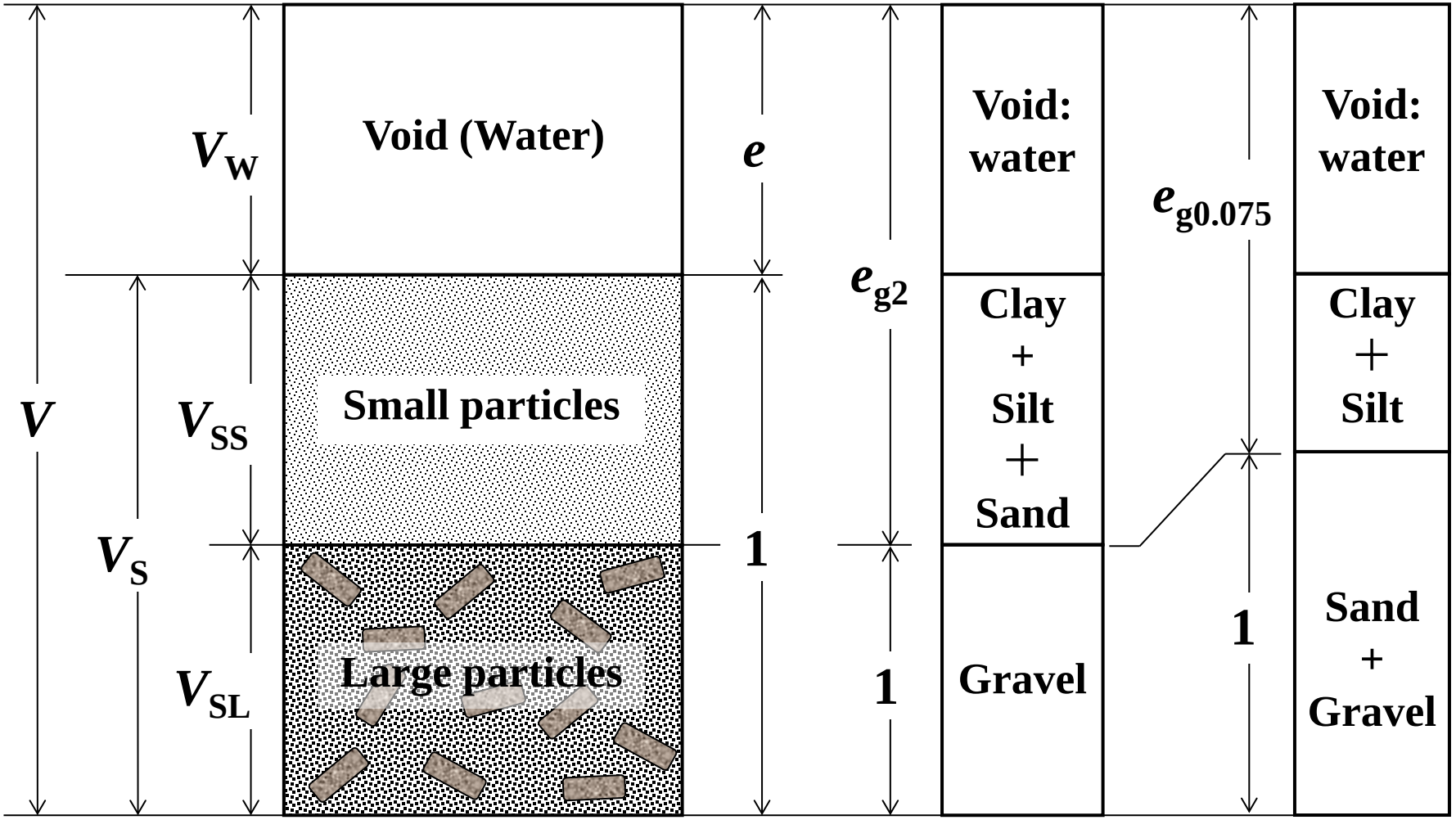
V_W
Void (Water)
e
Void: water
$e_{g0.075}$
Void: water
V
V_{SS}
Small particles
e_{g2}
Clay + Silt + Sand
Clay + Silt
V_S
1
1
1
V_{SL}
Large particles
Gravel
Sand + Gravel

a

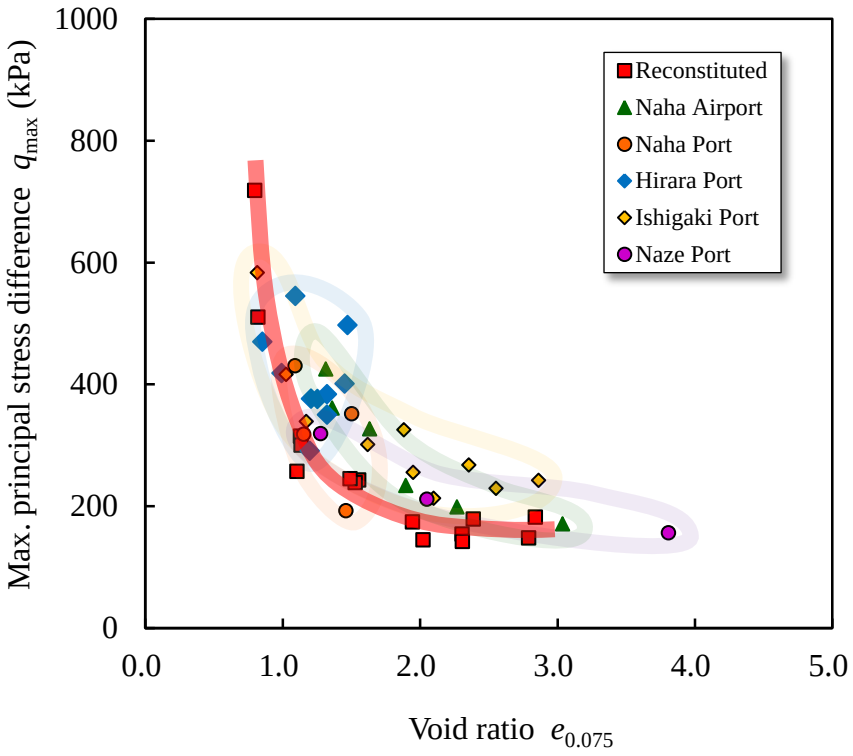
Max. principal stress difference q_{max} (kPa)
1000
800
600
400
200
0
0.0
1.0
2.0
3.0
4.0
5.0
Void ratio $e_{0.075}$
Reconstituted
Naha Airport
Naha Port
Hirara Port
Ishigaki Port
Naze Port

b

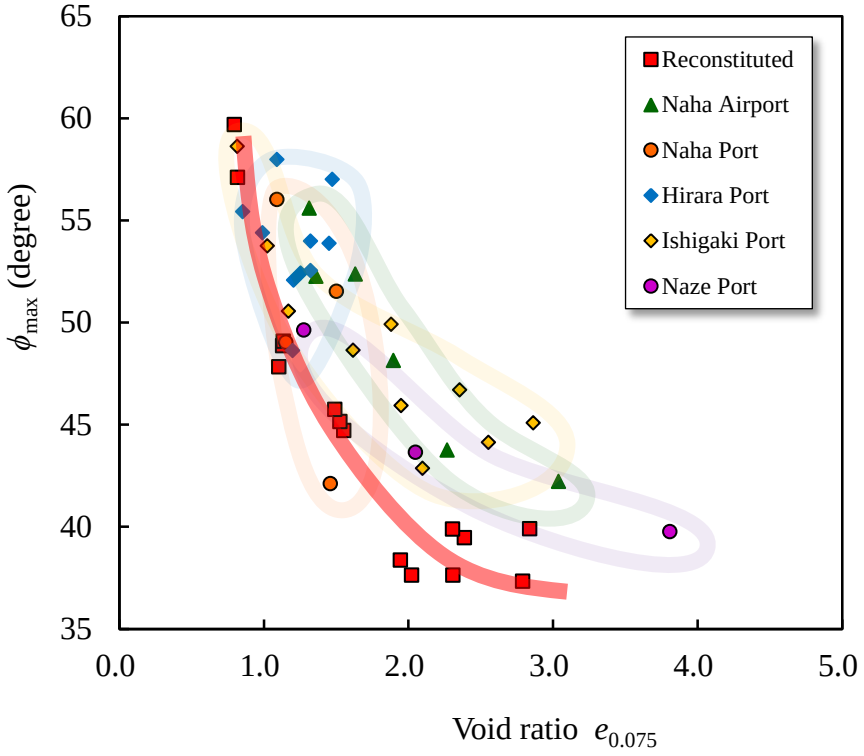
ϕ_{max} (degree)
65
60
55
50
45
40
35
0.0
1.0
2.0
3.0
4.0
5.0
Void ratio $e_{0.075}$
Reconstituted
Naha Airport
Naha Port
Hirara Port
Ishigaki Port
Naze Port

c

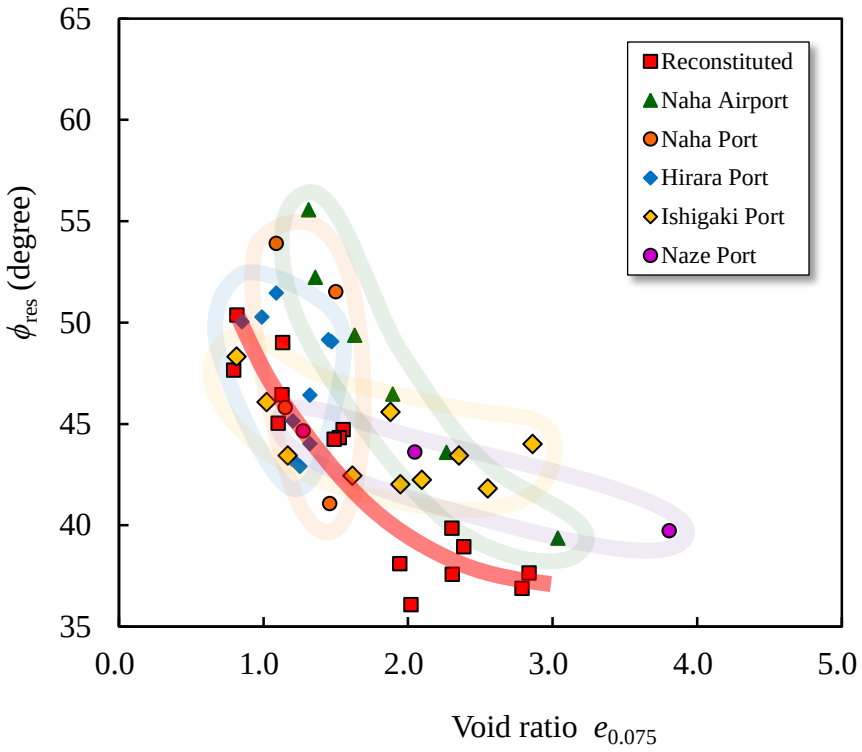
65
60
55
50
45
40
35
0.0
1.0
2.0
3.0
4.0
5.0
ϕ_{res} (degree)
Void ratio $e_{0.075}$
Reconstituted
Naha Airport
Naha Port
Hirara Port
Ishigaki Port
Naze Port

a

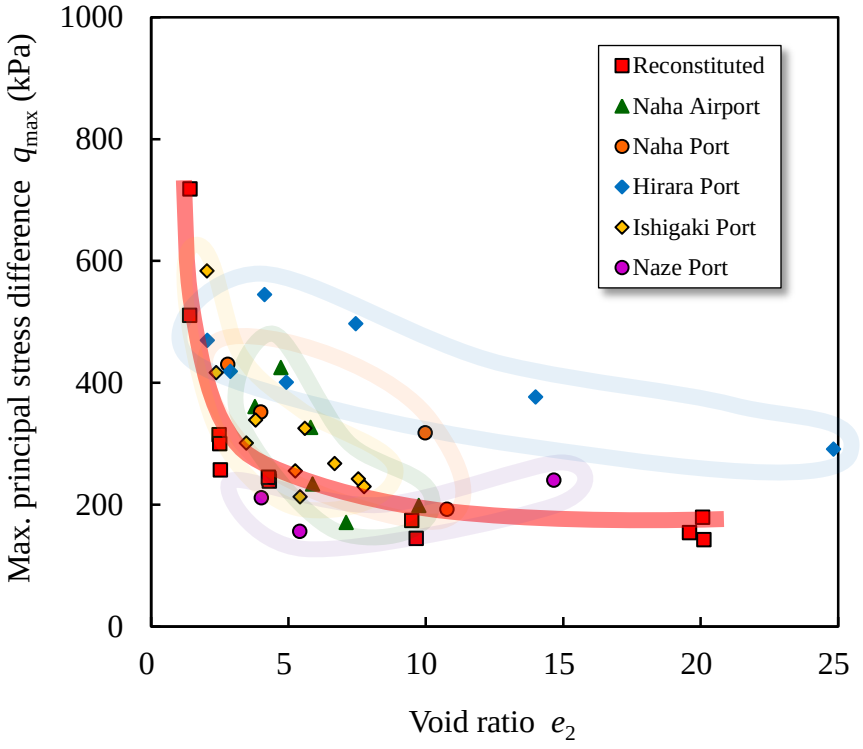
Max. principal stress difference q_{max} (kPa)
1000
800
600
400
200
0
0
5
10
15
20
25
Void ratio e_2
Reconstituted
Naha Airport
Naha Port
Hirara Port
Ishigaki Port
Naze Port

b

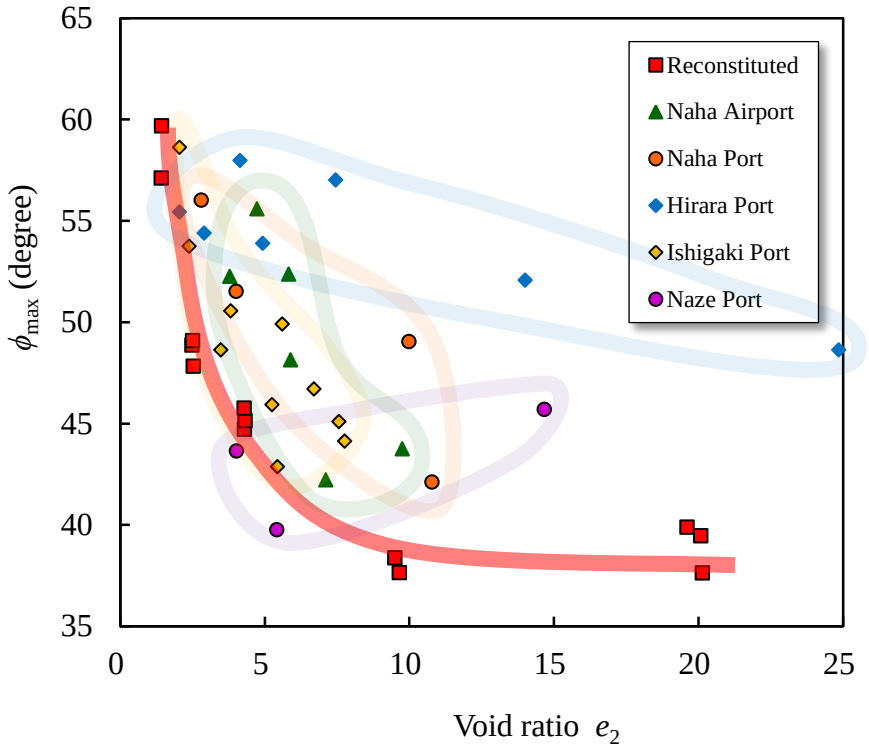
ϕ_{max} (degree)
65
60
55
50
45
40
35
0
5
10
15
20
25
Void ratio e_2
Reconstituted
Naha Airport
Naha Port
Hirara Port
Ishigaki Port
Naze Port

c

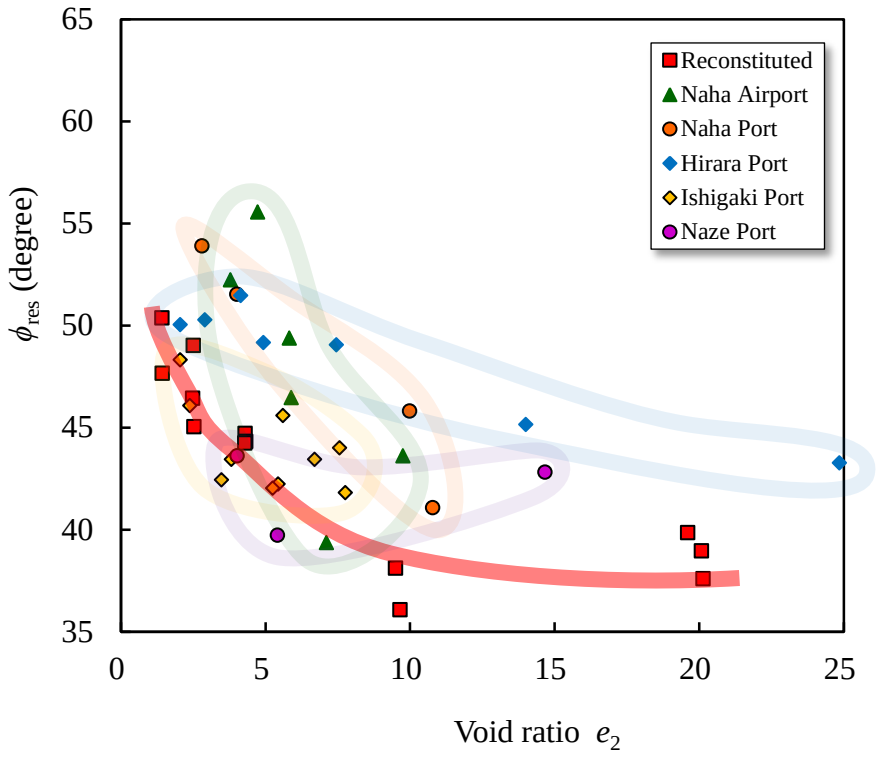
65
60
55
50
45
40
35
0
5
10
15
20
25
ϕ_{res} (degree)
Void ratio e_2
Reconstituted
Naha Airport
Naha Port
Hirara Port
Ishigaki Port
Naze Port

a

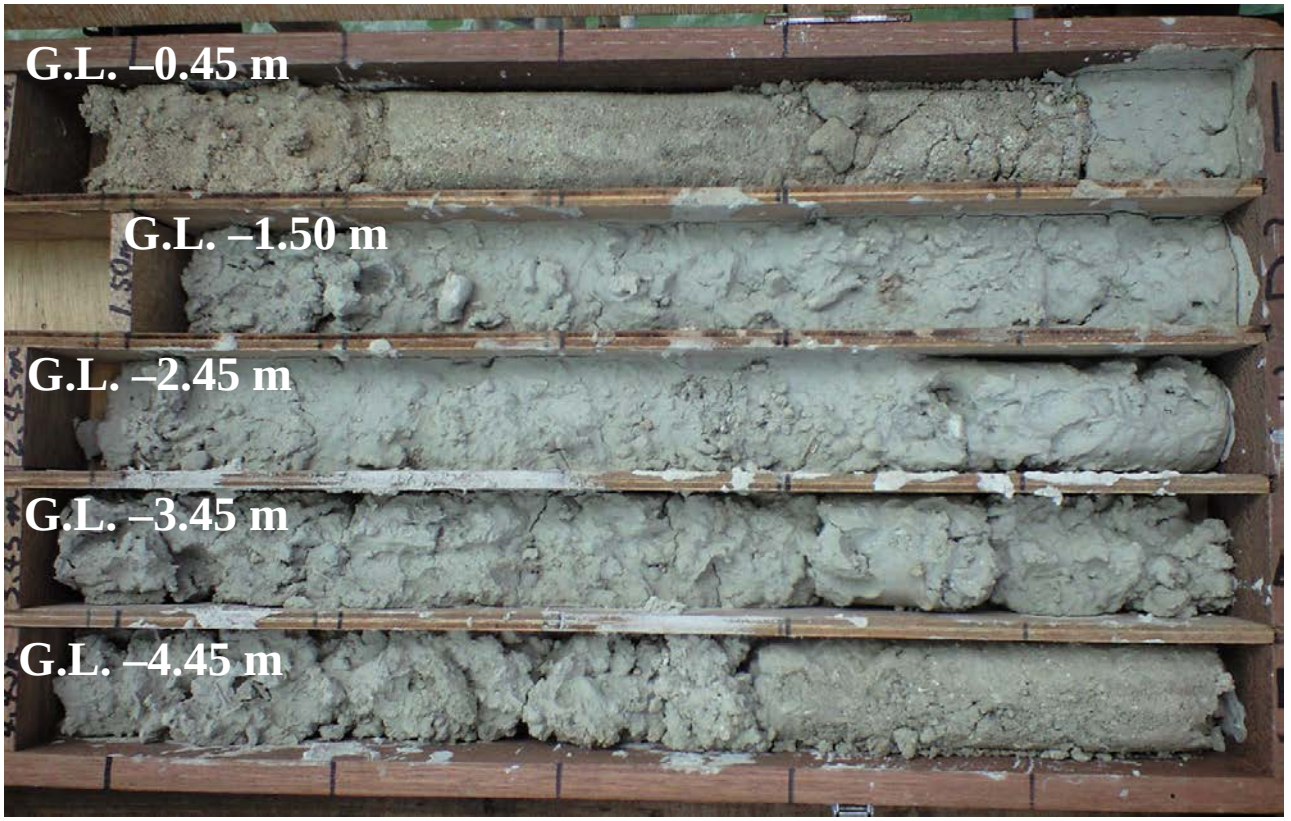
G.L. –0.45 m
G.L. –1.50 m
G.L. –2.45 m
G.L. –3.45 m
G.L. –4.45 m

b

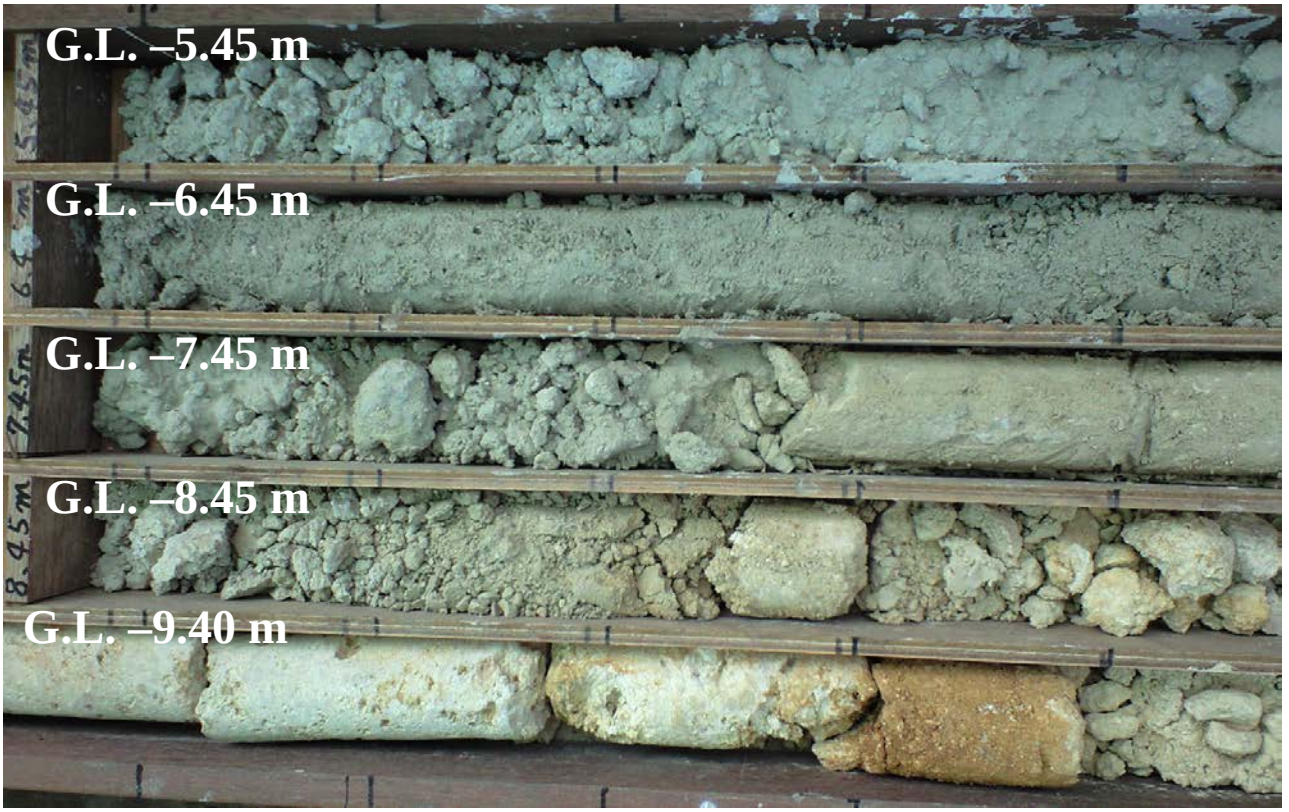
G.L. –5.45 m
G.L. –6.45 m
G.L. –7.45 m
G.L. –8.45 m
G.L. –9.40 m

BorNo.②

GS-5_0° 深度 (m) 11.00 ～ 11.95

0°

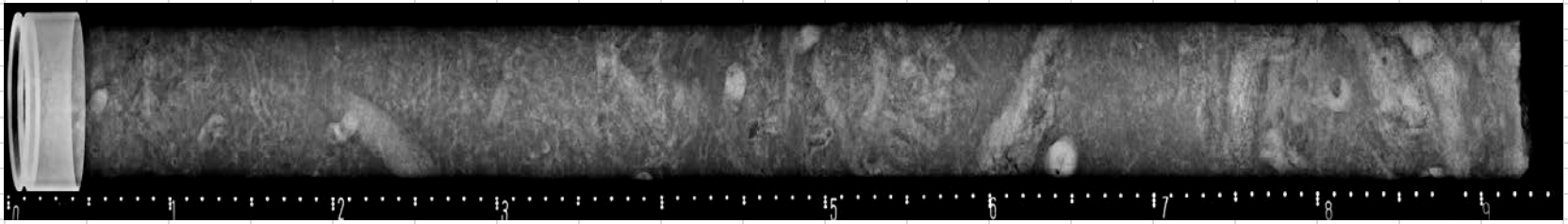

0 10 20 30 40 50 60 70 80 90 100

(11.95 m) (11.00 m)

BorNo.②

GS-5_90° 深度 (m) 11.00 ～ 11.95

90°

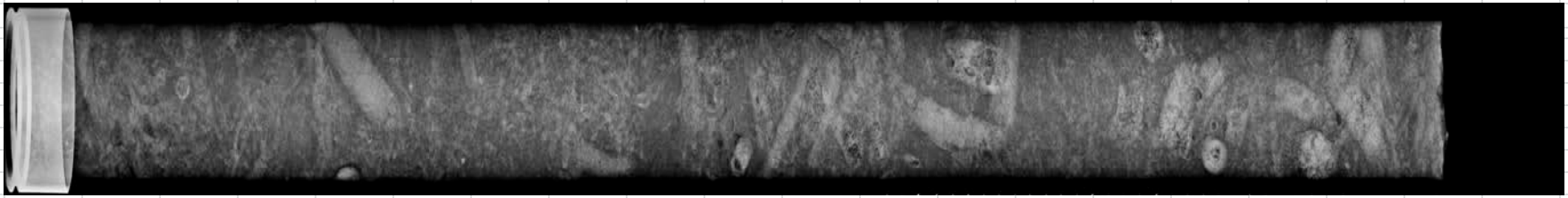

0 10 20 30 40 50 60 70 80 90 100

(11.95 m) (11.00 m)

a

b